Chapter 6

Design, synthesis and biological evaluation of *N-benzylpiperidines* as potential multitargeted ligands for the treatment of Alzheimer's disease

Summary:

Alzheimer's disease (AD) is a neurodegenerative disorder characterized by the accumulation of amyloid-β (Aβ) plaques and neurofibrillary tangles, leading to progressive cognitive impairment. The multi-faceted pathology of AD involves cholinergic deficits and increased activity of enzymes such as AChE and BACE-1. This study aimed to develop novel multi-target directed ligands (MTDLs) targeting both AChE and BACE-1 through a structure-based drug design approach utilizing N-*benzylpiperidine* scaffolds. Molecular docking studies revealed promising binding affinities and ligand efficiencies for the designed compounds against the target enzymes. *in-vitro* assays demonstrated potent inhibitory activities against AChE, and BACE-1, with notable structure-activity relationships. Selected compounds exhibited mixed type of AChE inhibition, dose-dependent inhibition of propidium iodide displacement from the AChE peripheral anionic site (PAS), and favorable blood-brain barrier permeation. Additionally, compounds **72** and **77** effectively inhibited AChE-induced $A\beta_{1-42}$ aggregation. *In-vivo* studies in rats revealed cognition-enhancing effects, reduction in AChE activity, and increased acetylcholine levels for compounds **72** and **77**. Furthermore, these compounds demonstrated protective effects against $A\beta_{1-42}$-induced memory deficits in the Morris water maze test. Overall, the findings support the potential of these MTDLs as promising therapeutic candidates for AD, warranting further preclinical and clinical evaluation.

6 Design, synthesis and biological evaluation of *N-benzylpiperidines* as potential multitargeted ligands for the treatment of Alzheimer's disease

6.1 Introduction

Dementia has emerged as a significant health and societal dilemma in contemporary times, and its impact is poised to deepen further as the global population ages. The number of individuals affected by dementia, with AD being the most prevalent form, is projected to surge dramatically from 35 million to a staggering 135 million by 2050. Currently, 60% of these cases are found in low- and middle-income countries, a percentage that is expected to increase to 71% by 2050 [101].

The absence of a cure exacerbates the challenges posed by AD. Although there are medications available, including three AChEI and memantine, they can only alleviate dementia symptoms and are incapable of halting the degenerative progression.

Recently, a novel approach known as multi-targeted inhibition has been embraced, aiming to simultaneously target multiple enzymes with a single molecule. This strategy is based on the understanding that AD is a complex disorder with involvement of multiple factors. Consequently, the design and development of multitarget-directed ligands hold great promise in effectively slowing down the progression of the disease rather than merely addressing its symptoms.

Among the various targets, AChE inhibition stands out as the most promising for improving cognitive dysfunctions exacerbated in AD. Additionally, BACE-1 inhibition is another crucial target, playing a significant role in cleaving APP, generating Aβ aggregates, and forming senile plaques. Furthermore, as Aβ is associated with oxidative damage, molecules with BACE-1 inhibitory potential may also exhibit substantial antioxidant effects.

Donepezil, the most potent AChE inhibitor, contains the N-benzylpiperidine nucleus as its core group, which binds to the catalytic active site (CAS) of AChE. The scientific literature also supports modifying the other terminal part (indanone nucleus) to enhance BACE-1 inhibitory potential.

Based on the information presented, it is proposed that ligands containing the N-benzylpiperidine nucleus could hold multi-functional enzyme inhibitory potential against both AChE and BACE-1, making them promising candidates for addressing AD.

Challenges in the development of new pharmacophores as therapeutics

The development of new pharmacophores as therapeutics presents several challenges, including:

Specificity and selectivity: Designing pharmacophores that selectively bind to the desired target while minimizing interactions with off-target proteins or receptors is a significant challenge. Lack of specificity can lead to undesirable side effects and reduced efficacy.

Bioavailability and pharmacokinetics: Ensuring adequate absorption, distribution, metabolism, and excretion (ADME) properties is crucial for pharmacophores to reach their target site and maintain effective concentrations. Poor bioavailability or unfavorable pharmacokinetics can limit the therapeutic potential of a pharmacophore.

Blood-brain barrier (BBB) permeability: For pharmacophores targeting the central nervous system (CNS), crossing the BBB is a major obstacle. The BBB is a selective barrier that protects the brain from potentially harmful substances, making it difficult for many compounds to reach their intended targets in the brain.

Toxicity and safety concerns: Thorough evaluation of potential toxicity and safety issues is necessary during the development process. Pharmacophores with unacceptable toxicity profiles or safety risks may need to be modified or abandoned.

Synthetic accessibility and scalability: The synthesis of pharmacophores, especially complex molecules, can be challenging and may require extensive optimization to achieve efficient and scalable synthetic routes for large-scale production.

Resistance and potential for off-target effects: Developing pharmacophores that can overcome resistance mechanisms and minimize off-target effects is crucial, particularly in areas such as antimicrobial and anticancer drug development.

Intellectual property considerations: Navigating the intellectual property landscape and ensuring freedom to operate for new pharmacophores can be a complex process, requiring careful evaluation of existing patents and potential infringement issues.

6.2 Design aspects

The design strategy for multitarget-directed *N-benzylpiperidins* was based on hybrid pharmacophore approach. The cholinergic and Amyloid-ß ($Aß_{1-42}$) hypothesis are key approaches to treat AD. A set of MTDLs was generated as the structural template of donepezil, the most potent and widely prescribed drug for treating advanced-stage AD [102]. An exploration of the Structure-Activity Relationship (SAR) of donepezil revealed a substantial reduction in AChE inhibitory activity upon modifications or substitutions in the benzyl portion of the *N-benzylpiperidine* moiety. Additionally, the *N-benzylpiperidine* ring of donepezil was found to extend into the catalytic anionic site (CAS), while the terminal indanone nucleus was positioned in the Peripheral Anionic Site (PAS) of AChE [102]. Furthermore, the *N-benzylpiperidine* ring contains a basic nitrogen moiety that becomes protonated at physiological pH, enhancing affinity towards AChE and the aspartate dyad of BACE-1 and demonstrating significant blood-brain barrier (BBB) permeability due to acid-base equilibrium (23). These encouraging findings motivated the selection of the *N-benzylpiperidine* nucleus as a core group for designing novel hybrid compounds (**Figure 6.1**). The *N-benzylpiperidine* was chosen as an initial prompt and

then was the molecule was allowed to grow and new molecules were generated using CReM structure generation tool [103]. The generated molecules were then subject to ML-based screening using previously developed models. This led to the identification of a hit, which was further optimized.

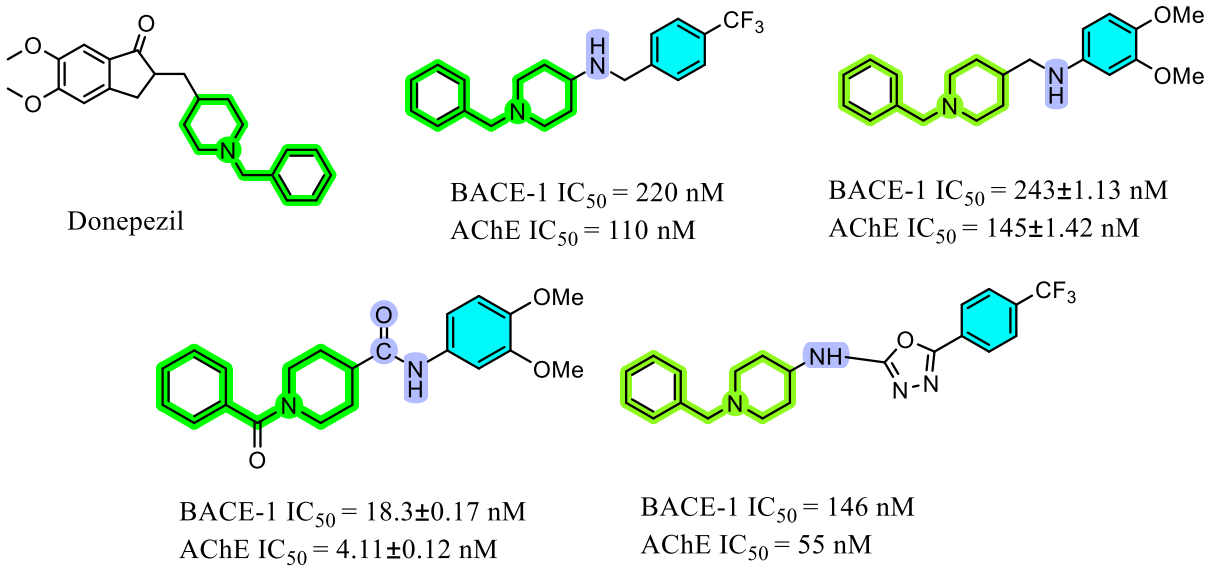

Figure 6.1 N-benzylpiperidines as AChE and BACE-1 inhibitors

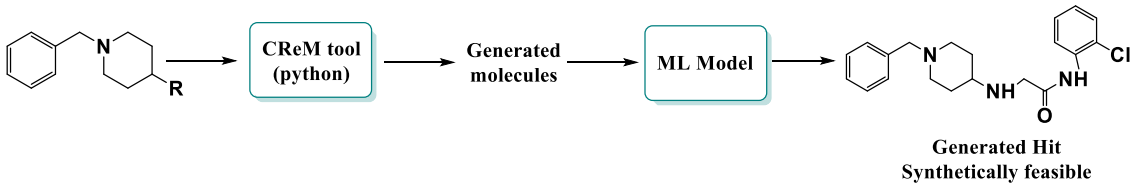

Figure 6.2 Workflow of molecule generation tool

6.3 Material and methods

6.3.1 Docking studies

The designed molecules were docked against AChE and BACE-1 using Autodock. The 3D coordinates of ligands were created using Rdkit based on the SMILES strings of the compounds. Subsequently, energy minimization was performed utilizing the MMFF94s

forcefield, and the results were then transformed into Mol2 format using Open Babel. Subsequently, Autodock Tools-1.5.6 was used to convert the ligands to PDBQT format.

6.3.1.1 Docking study with AChE

PLIP was employed to pinpoint residues involved in non-covalent interactions with donepezil within the chosen PDB file (4ey7). These identified residues were used as a basis to create a grid box encompassing the active site. Autogrid 4.0 was then employed to compute grid maps detailing interaction energies concerning various atom types found in ligands (A, C, HD, NA, N, OA, S, Br, Cl, and I). The grid dimensions were configured at 74 × 70 × 82, with a grid point spacing of 0.375 Å. The Lamarckian Genetic Algorithm (LGA) was employed for conformational search. The number of GA runs was set to 50, the population size was set to 150, the maximum number of generations was set to 270000 and the maximum number of evaluations was set to 2500000.

6.3.1.2 Docking study with BACE-1

The docking protocol has been described in section **4.2.7**.

6.3.2 Molecular property and toxicity prediction

Molecular characteristics, including cLogP, cLogS, hydrogen bond acceptor, donor, and drug-likeness, were examined using DataWarrior in accordance with Lipinski's rule of five. Our previous model was utilized to perform BBB permeability *in-silico*. Hazardousness, mutagenicity, tumorigenicity, and irritancy of compounds in the investigation were also forecast using OSIRIS DataWarrior [81].

6.3.3 *In-silico* ADME property analysis

The *in-silico* ADME property analysis was performed using the SWISS ADME web-server accessible at http://www.swissadme.ch [104]. The following properties were calculated viz. Aqueous solubility, GI absorption, BBB permeant, CYP2C9 inhibitor, CYP2D6 inhibitor, CYP3A4 inhibitor and PAINS alerts.

6.3.4 Synthesis and Characterization

We procured analytical grade chemicals and solvents from various suppliers, including Avera, Alfa Acer, Merck, Sigma Aldrich, and SD. To monitor the progress of chemical reactions, we employed thin-layer chromatography (TLC) using pre-coated silica gel 60 F254 plates from Merck KGaA. Visualization was achieved using either ultraviolet light at 254 nm or iodine vapors. To purify the compounds, we utilized column chromatography with silica gel (60-120 mesh size). Melting points were determined using an automated melting point system (Barnstead Electrothermal, UK).

For spectroscopic analysis, we recorded IR(ATR) spectra on a Bruker FTIR spectrometer Alpha T (Germany). Additionally, 1H and 13C NMR spectra were acquired in DMSO-d6 on a Bruker 500 FTNMR spectrometer operating at frequencies of 500 and 125 MHz, respectively. The coupling constant (J) was measured in Hz, and the chemical shift (δ) was estimated in ppm.

Mass spectra were collected using a UPLC/XEVO G2-XS QTOF apparatus equipped with APCI and ESI multi-mode ionization sources. To assess compound purity, we employed an Agilent 1260 Infinity II Quaternary LC system with a DAD HS G7115A detector operating at a wavelength of 315 nm. The isocratic mobile phase consisted of acetonitrile (phase A) and methanol (phase B) in a 1:9 ratio, delivered by quaternary pumps at a flow rate of 1 ml/min. Samples of 20 µL were injected into the HPLC column, and detection was performed at 315 nm wavelength using an SPD10AVP detector.

The purification process utilized a CLC C18 column (5µ, 25 cm × 4.6 mm i.d) with a CLC ODS guard column (4 cm × 4.6 mm i.d).

6.3.4.1 General procedure for synthesis of derivatives of *2-chloro-N-phenylacetamide* (30-57)

Substituted aniline (1.7 mmol, 1 equivalent) was dissolved in DCM (5ml) and triethyl amine (2.5 equivalent) was added. The solution was placed over the ice bath, and drop by drop, chloroacetylchloride (1.7 mmol, 1 equivalent) was added to the solution with continuous stirring. The reaction mixture was stirred at room temperature for 1 hr. Precipitate was obtained after the addition of chloroacetylchloride in the RBF. The reaction was quenched with water (30 mL), and the mixture was extracted with DCM and washed with saturated ammonium chloride. The combined organic layer was dried over sodium sulfate. The organic layer was evaporated under reduced pressure through a rotary evaporator. The intermediate formed was checked through TLC using the ethylacetate and hexane (7:3) as the mobile phase.

***2-chloro-N-phenylacetamide* (30)**

White Solid (0.499g, 93.75% yield) M.P:163-167°C, Rf=0.86 (EA/Hex,7:3,v/v). IR(ATR): 1651 (C=0 stretching), 3345 (Secondary NH stretching), 2956 (C-H stretching), 1170 (C-N stretching) cm^{-1}. ^{1}H NMR (500 MHz, DMSO-d6) δ 8.62 – 8.59 (NH,s, 1H), 7.55 – 7.49 (Ar-H,m, 2H), 7.47 – 7.40 (Ar-H,m, 2H), 7.17 – 7.11 (Ar-H,m, 1H), 4.23 – 4.19 (CH2,s, 2H). 13C NMR (125 MHz, DMSO-d6) δ 167.69, 137.76, 129.31, 123.72, 121.46, 41.74.

***2-chloro-N-(2-nitrophenyl)acetamide* (31)**

Grey Solid (0.670g, 96.76% yield) M.P: 98-100°C, Rf=0.83 (EA/Hex,7:3,v/v). IR(ATR) : 1650 (C=0 stretching), 3210(Secondary NH stretching), 2977(C-H stretching), 1240 (C-N stretching) cm^{-1}. ^{1}H NMR (500 MHz, DMSO-d6) δ 9.68 – 9.64 (NH,s, 1H), 8.28 – 8.22 (Ar-H,m, J = 9.0, 1.4 Hz, 1H), 7.97 – 7.91 (Ar-H,m, J = 7.5, 1.5 Hz, 1H), 7.75 – 7.68 (Ar-

H,td, J = 7.8, 1.5 Hz, 1H), 7.42 – 7.35 (Ar-H,m, 1H), 4.23 – 4.20 (CH_2,s, 2H). 13C NMR (125 MHz, DMSO-d6) δ 168.03, 136.51, 135.90, 133.67, 127.13, 124.07, 124.04, 41.74.

2-chloro-N-(3-nitrophenyl)acetamide **(32)**

Pale Yellow Solid (0.652g, 98.54% yield) M.P: 113-117°C, Rf=0.83 (EA/Hex, 7:3,v/v). IR (ATR) : 1647 (C=0 stretching), 3310(Secondary NH stretching), 2951(C-H stretching), 1242 (C-N stretching) cm^{-1}. ^1H NMR (500 MHz, DMSO-d6) δ 9.68 – 9.65 (s, 1H), 8.52 – 8.48 (t, J = 2.2 Hz, 1H), 8.46 – 8.40 (m, J = 7.9, 1.9, 1.0 Hz, 1H), 7.76 – 7.70 (m, J = 7.9, 2.4, 0.9 Hz, 1H), 7.60 – 7.53 (t, J = 8.0 Hz, 1H), 4.23 – 4.19 (s, 2H). 13C NMR (125 MHz, DMSO-d6) δ 167.69, 148.70, 139.64, 129.27, 127.01, 120.28, 115.89, 41.74.

2-chloro-N-(4-nitrophenyl)acetamide **(33)**

Yellow Solid (0.596g, 91% yield) M.P: 100-103°C, Rf=0.88 (EA/Hex,7:3,v/v). IR(ATR) : 1652(C=0 stretching), 3218(Secondary NH stretching), 2951(C-H stretching), 1223 (C-N stretching) cm^{-1}. ^1H NMR (500 MHz, DMSO-d6) δ 9.48 – 9.44 (NH,s, 1H), 8.22 – 8.16 (Ar-H,m, 2H), 7.83 – 7.77 (Ar-H,m, 2H), 4.23 – 4.19 (CH2,s, 2H). 13C NMR (125 MHz, DMSO-d6) δ 167.69, 145.42, 144.14, 125.54, 120.66, 41.74.

N-(2-bromophenyl)-2-chloroacetamide **(34)**

Grey Solid (0.575g, 98.61% yield) M.P: 88-92°C, Rf=0.9 (EA/Hex,7:3,v/v). IR(ATR) : 1654 (C=0 stretching), 3243(Secondary NH stretching), 2950(C-H stretching), 1215 (C-N stretching) cm^{-1}. ^1H NMR (500 MHz, DMSO-d6) δ 8.94 – 8.91 (NH,s, 1H), 7.70 – 7.64 (Ar-H,m, J = 7.7, 1.4 Hz, 1H), 7.56 – 7.50 (Ar-H,m, J = 8.1, 1.4 Hz, 1H), 7.35 – 7.28 (Ar-H,td, J = 7.4, 1.4 Hz, 1H), 7.27 – 7.20 (Ar-H,m, 1H), 4.23 – 4.20 (CH2,s, 2H). 13C NMR (125 MHz, DMSO-d6) δ 168.03, 138.33, 133.51, 128.47, 125.51, 123.39, 113.90, 41.74.

N-(3-bromophenyl)-2-chloroacetamide **(35)**

White Solid (0.498g, 95.78%yield) M.P:110-114°C , Rf=0.75 (EA/Hex,7:3,v/v). IR(ATR) : 1661 (C=0 stretching), 3276(Secondary NH stretching), 2951(C-H stretching), 1246 (C-N stretching) cm^{-1}. ^{1}H NMR (500 MHz, DMSO-d6) δ 9.18 – 9.14 (NH,s, 1H), 7.89 – 7.85 (Ar-H,t, J = 2.1 Hz, 1H), 7.46 – 7.40 (Ar-H,m, J = 7.9, 2.2, 1.3 Hz, 1H), 7.33 – 7.27 (Ar-H,m, J = 7.7, 2.1, 1.2 Hz, 1H), 7.26 – 7.19 (Ar-H,d, J = 15.6 Hz, 1H), 4.23 – 4.19 (CH2,s, 2H). ^{13}C NMR (125 MHz, DMSO-d6) δ 167.69, 139.30, 130.42, 127.62, 122.67, 121.91, 120.63, 41.74.

N-(4-bromophenyl)-2-chloroacetamide **(36)**

Grey Solid (0.440g, 93.34% yield) M.P: 118-121°C, Rf=0.86 (EA/Hex, 7:3,v/v). IR (ATR): 1653 (C=0 stretching), 3338(Secondary NH stretching), 2955(C-H stretching), 1157 (C-N stretching) cm^{-1}. ^{1}H NMR (500 MHz, DMSO-d6) δ 9.16 – 9.12 (NH,s, 1H), 7.53 – 7.43 (Ar-H,m, 4H), 4.23 – 4.19 (CH2,s, 2H). 13C NMR (125 MHz, DMSO-d6) δ 167.69, 136.21, 131.79, 122.19, 118.25, 41.74.

2-chloro-N-(2-fluorophenyl)acetamide **(37)**

White Solid (0.378g, 89.21% yield) M.P: 165-168°C, Rf= 0.8(EA/Hex, 7:3,v/v).IR(ATR) : 1650 (C=0 stretching), 3303(Secondary NH stretching), 2962(C-H stretching), 1173 (C-N stretching) cm^{-1}. ^{1}H NMR (500 MHz, DMSO-d6) δ 9.34 – 9.31 (NH,s, 1H), 7.50 – 7.44 (Ar-H,m, J = 7.7, 2.2, 1.1 Hz, 1H), 7.35 – 7.25 (Ar-H,m, 2H), 6.92 – 6.84 (Ar-H,m, J = 9.9, 7.7, 2.1, 1.1 Hz, 1H), 4.23 – 4.19 (CH2,s, 2H). 13C NMR (125 MHz, DMSO-d6) δ 168.03, 156.32, 125.85, 125.69, 125.19, 124.28, 117.10, 41.74.

2-chloro-N-(3-fluorophenyl)acetamide **(38)**

White Solid (0.595g, 99.10 % yield) M.P: 161-163°C, Rf=0.83 (EA/Hex,7:3,v/v).IR(ATR) : 1672 (C=0 stretching), 3309(Secondary NH stretching), 2975(C-H stretching), 1161 (C-N stretching) cm^{-1}. ^{1}H NMR (500 MHz, DMSO-d6) δ 9.34 – 9.31 (NH,s, 1H), 7.50 – 7.44 (Ar-H,m, J = 7.7, 2.2, 1.1 Hz, 1H), 7.35 – 7.25 (Ar-

H,m, 2H), 6.92 – 6.84 (Ar-H,m, J = 9.9, 7.7, 2.1, 1.1 Hz, 1H), 4.23 – 4.19 (CH2,s, 2H). 13C NMR (125 MHz, DMSO-d6) δ 167.69, 163.12, 140.00, 130.05, 117.04, 112.15, 109.08, 41.74.

***2-chloro-N-(4-fluorophenyl)acetamide* (39)**

Pale Pink Solid (0.403g, 90.75% yield) M.P: 179-182°C, Rf=0.77 (EA/Hex,7:3,v/v). IR(ATR) : 1667 (C=0 stretching), 3272(Secondary NH stretching), 2950(C-H stretching), 1165 (C-N stretching) cm^{-1}. ^{1}H NMR (500 MHz, DMSO-d6) δ 9.21 – 9.17 (NH,s, 1H), 7.53 – 7.47 (Ar-H,m, 2H), 7.19 – 7.11 (Ar-H,m, 2H), 4.23 – 4.19 (CH2,s, 2H). 13C NMR (125 MHz, DMSO-d6) δ 167.69, 159.97, 134.73, 122.58, 116.47, 41.74.

***2-chloro-N-(o-tolyl)acetamide* (40)**

Pale Pink Solid (0.499g, 96.58% yield) M.P: 132-135°C, Rf=0.78 (EA/Hex,7:3,v/v). IR(ATR):1644 (C=0 stretching), 3268(Secondary NH stretching), 2973(C-H stretching), 1172 (C-N stretching) cm^{-1}. ^{1}H NMR (500 MHz, DMSO-d6) δ 8.25 – 8.21 (NH,s, 1H), 7.51 – 7.41 (Ar-H,m, 2H), 7.28 – 7.19 (Ar-H,m, 2H), 4.24 – 4.20 (CH2,s, 2H). 13C NMR (125 MHz, DMSO-d6) δ 168.03, 137.43, 131.80, 130.03, 127.54, 124.96, 122.76, 41.74, 17.35.

***2-chloro-N-(m-tolyl)acetamide* (41)**

Dark Brown Solid (0.321g, 88.46% yield) M.P: 142-144°C, Rf=0.77 (EA/Hex,7:3,v/v). IR (ATR) : 1648 (C=0 stretching), 3239(Secondary NH stretching), 2970(C-H stretching), 1176 (C-N stretching) cm^{-1}. ^{1}H NMR (500 MHz, DMSO-d6) δ 8.68 – 8.65 (NH,s, 1H), 7.51 – 7.43 (Ar-H,m, 2H), 7.18 – 7.12 (Ar-H,d, J = 7.6 Hz, 1H), 6.97 – 6.91 (Ar-H,m, 1H), 4.23 – 4.19 (CH2,s, 2H), 2.31 – 2.27 (CH3,d, J = 0.7 Hz, 3H). 13C NMR (125 MHz, DMSO-d6) δ 167.69, 139.50, 138.32, 128.94, 126.50, 120.29, 119.22, 41.74, 21.21.

***2-chloro-N-(p-tolyl)acetamide* (42)**

Grey Solid (0.428g, 91.17% yield) M.P: 149-151°C, Rf=0.88 (EA/Hex,7:3,v/v). IR(ATR) : 1658 (C=0 stretching), 3281(Secondary NH stretching), 2951(C-H stretching), 1233 (C-N stretching) cm^{-1}. ^1H NMR (500 MHz, DMSO-d6) δ 9.12 – 9.09 (NH,s, 1H), 7.45 – 7.39 (Ar-H,m, 2H), 7.16 – 7.10 (Ar-H,m, 2H), 4.23 – 4.19 (CH2,s, 2H), 2.37 – 2.33 (CH3,s, 3H). 13C NMR (125 MHz, DMSO-d6) δ 167.69, 136.58, 133.31, 129.75, 119.33, 41.74, 21.13.

***2-chloro-N-(2-chlorophenyl)acetamide* (43)**

Dark Brown Solid (0.378g, 88.47% yield) M.P: 134-136°C, Rf=0.85 (EA/Hex,7:3,v/v).IR(ATR) : 1646 (C=0 stretching), 3337(Secondary NH stretching), 2954(C-H stretching), 1237 (C-N stretching) cm^{-1}. ^1H NMR (500 MHz, DMSO-d6) δ 8.97 – 8.94 (NH,s, 1H), 7.50 – 7.45 (Ar-H,m, J = 7.9, 1.4 Hz, 1H), 7.42 – 7.35 (Ar-H,m, 1H), 7.28 – 7.22 (Ar-H,m, 1H), 7.11 – 7.04 (Ar-H,m, J = 8.3, 7.1, 1.4 Hz, 1H), 4.23 – 4.20 (CH2,s, 2H). 13C NMR (125 MHz, DMSO-d6) δ 168.03, 135.66, 130.62, 128.23, 128.05, 126.11, 124.73, 41.74.

***2-chloro-N-(3-chlorophenyl) acetamide* (44)**

Grey Solid (0.448g, 95.76% yield) M.P: 174-177°C, Rf=0.89 (EA/Hex,7:3,v/v).IR(ATR) : 1654 (C=0 stretching), 3220(Secondary NH stretching), 2958(C-H stretching), 1200 (C-N stretching) cm^{-1}. ^1H NMR (500 MHz, DMSO-d6) δ 9.18 – 9.15 (NH,s, 1H), 7.56 – 7.51 (Ar-H,t, J = 2.1 Hz, 1H), 7.47 – 7.41 (Ar-H,m, J = 8.0, 2.1, 1.2 Hz, 1H), 7.35 – 7.28 (Ar-H,d, J = 15.8 Hz, 1H), 7.19 – 7.13 (Ar-H,m, J = 7.9, 2.2, 1.3 Hz, 1H), 4.23 – 4.19 (CH2,s, 2H). 13C NMR (125 MHz, DMSO-d6) δ 167.69, 139.54, 134.34, 129.90, 124.84, 120.45, 120.38, 41.74.

***2-chloro-N-(4-chlorophenyl)acetamide* (45)**

Pale Brown Solid (0.403g, 90.54% yield), M.P:149-151°C, Rf=0.78 (EA/Hex,7:3,v/v). IR(ATR) : 1649 (C=0 stretching), 3253(Secondary NH stretching), 2971(C-H stretching),

1156 (C-N stretching) cm^{-1}. ^{1}H NMR (500 MHz, DMSO-d6) δ 9.27 – 9.24 (NH,s, 1H), 7.62 – 7.57 (Ar-H,m, 2H), 7.38 – 7.33 (Ar-H,m, 2H), 4.23 – 4.19 (CH2,s, 2H). 13C NMR (125 MHz, DMSO-d6) δ 167.69, 136.53, 129.24, 128.63, 122.21, 41.74.

***2-chloro-N-(2-methoxyphenyl) acetamide* (46)**

Grey Solid (0.475g, 95.10 % yield) M.P: 132-133°C, Rf=0.73 (EA/Hex,7:3,v/v). ^{1}H NMR (500 MHz, DMSO-d6) *δ* 8.32 (dd, *J = 7.9, 1.5 Hz*, 1H), 8.28 (s, 1H), 7.09 (td, *J = 8.0*, 1.5 Hz, 1H), 7.03 (td, *J = 8.0*, 1.4 Hz, 1H), 6.93 (dd, *J = 8.0*, 1.3 Hz, 1H), 4.22 (s, 2H), 3.93 (s, 3H). ^{13}C NMR (125 MHz, DMSO-d6) *δ* 165.29, 150.52, 128.66, 122.28, 121.76, 120.75, 110.66, 55.69, 43.01.

***2-chloro-N-(3-methoxyphenyl) acetamide* (47)**

Brown Solid (0.410 g, 98.14 % yield) M.P: 137-139°C, Rf=0.78 (EA/Hex,7:3,v/v).^{1}H NMR (500 MHz, DMSO-d6) *δ* 9.24 (s, 1H), 7.30 – 7.28 (m, 1H), 7.28 (d, *J = 1.5 Hz*, 1H), 7.26 – 7.22 (m, 1H), 7.08 – 7.06 (m, 1H), 4.21 (s, 2H), 3.82 (s, 3H). ^{13}C NMR (125 MHz, DMSO-d6) *δ* 165.30, 160.33, 139.80, 130.02, 113.46, 111.24, 106.17, 55.59, 43.38.

***2-chloro-N-(4-methoxyphenyl) acetamide* (48)**

Brown Solid (0.572g, 94.10 % yield) M.P: 134-135°C, Rf=0.83 (EA/Hex,7:3,v/v). ^{1}H NMR (500 MHz, DMSO-d6) *δ* 9.26 (s, 1H), 8.33 (d, *J = 1.3 Hz*, 1H), 8.31 (d, *J = 1.5 Hz*, 1H), 6.97 (d, *J = 1.3 Hz*, 1H), 6.96 (d, *J = 1.5 Hz*, 1H), 4.21 (s, 2H), 3.80 (s, 3H). ^{13}C NMR (125 MHz, DMSO-d6) *δ* 164.92, 156.42, 133.16, 122.30, 112.27, 55.35, 43.57.

***2-chloro-N-(2-cyanophenyl)acetamide* (49)**

Grey Solid (0.499g, 95.21% yield)M.P: 140-142°C, Rf= 0.82(EA/Hex,7:3,v/v). IR(ATR): 1642 (C=0 stretching), 3307 (Secondary NH stretching), 2963(C-H stretching), 1244 (C-N stretching) cm^{-1}. ^{1}H NMR (500 MHz, DMSO-d6) δ 8.90 – 8.86 (NH,s, 1H), 7.75 – 7.70 (Ar-H,m, J = 6.6, 1.3 Hz, 1H), 7.69 – 7.64 (Ar-H,m, J = 7.9, 1.4 Hz, 1H), 7.49 – 7.42 (Ar-H,m, J = 8.0, 6.9, 1.4 Hz, 1H), 7.27 – 7.20 (Ar-H,m, 1H), 4.23 – 4.20 (CH2,s,

2H). 13C NMR (125 MHz, DMSO-d6) δ 168.03, 141.08, 133.62, 132.59, 122.41, 121.15, 117.68, 97.59, 41.74.

***2-chloro-N-(3-cyanophenyl)acetamide* (50)**

Brown Solid (0.378g, 89.52% yield) M.P: 167-171°C, Rf=0.79 (EA/Hex,7:3,v/v). IR(ATR): 1664 (C=0 stretching), 3264(Secondary NH stretching), 2972(C-H stretching), 1215 (C-N stretching) cm^{-1}.^{1}H NMR (500 MHz, DMSO-d6) δ 9.29 – 9.25 (NH,s, 1H), 7.93 – 7.88 (Ar-H,m, 1H), 7.83 – 7.76 (Ar-H,m, 1H), 7.47 – 7.40 (Ar-H,m, 2H), 4.23 – 4.19 (CH2,s, 2H). 13C NMR (125 MHz, DMSO-d6) δ 167.69, 139.27, 130.61, 129.90, 127.19, 123.07, 119.29, 111.12, 41.74. ***2-chloro-N-(4-cyanophenyl)acetamide* (51)**

Brown Solid (0.403g, 90.75% yield) M.P: 147-150°C, Rf=0.89 (EA/Hex,7:3,v/v). IR(ATR) : 1670 (C=0 stretching), 3340(Secondary NH stretching), 2964(C-H stretching), 1226 (C-N stretching) cm^{-1}. ^{1}H NMR (500 MHz, DMSO-d6) δ 9.18 – 9.15 (NH,s, 1H), 7.75 – 7.69 (Ar-H,m, 2H), 7.64 – 7.58 (Ar-H,m, 2H), 4.23 – 4.19 (CH2,s, 2H). 13C NMR (125 MHz, DMSO-d6) δ 167.69, 140.74, 131.79, 121.81, 119.12, 105.57, 41.74. MS (EI+): m/z calculated for C9H7ClN2O, found -194.02 (M^+).

***2-chloro-N-(2-(trifluoromethyl) phenyl) acetamide* (52)**

Pale Brown Solid (0.310 g, 94.54% yield), M.P:157-158°C, Rf=0.64 (EA/Hex,6:4,v/v). ^{1}H NMR (500 MHz, DMSO-d6) δ 9.66 (s, 1H), 7.95 (dd, J = 7.1, 1.5 Hz, 1H), 7.71 (dt, J = 10.6, 1.4 Hz, 1H), 7.48 – 7.44 (m, 1H), 7.37 (td, J = 7.2, 1.4 Hz, 1H), 4.22 (s, 3H). 13C NMR (125 MHz, DMSO-d6) δ 165.38, 137.85, 129.31, 127.50, 124.58, 122.34, 121.94, 121.04, 42.96.

***2-chloro-N-(4-(trifluoromethyl) phenyl) acetamide* (53)**

Pale Brown Solid (0.372 g, 97.41% yield), M.P:151-154°C, Rf=0.71 (EA/Hex,6:4,v/v) 1H NMR (500 MHz, DMSO-d6) δ 9.15 (s, 1H), 7.75 (d, J = 7.3 Hz, 2H), 7.56 (dq, J =

7.3, 1.3 Hz, 2H), 4.21 (s, 2H). 13C NMR (125 MHz, DMSO-d6) δ 164.92, 138.69, 126.84, 126.80, 125.52, 122.64, 120.48, 120.45, 43.57.

***2-chloro-N-(3-(trifluoromethyl) phenyl) acetamide* (54)**

Pale Brown Solid (0.410 g, 94.46 % yield), M.P:154-156°C, Rf=0.60 (EA/Hex,6:4,v/v) ^{1}H NMR (500 MHz, DMSO-d6) δ 9.32 (s, 1H), 7.86 (t, J = 2.0 Hz, 1H), 7.58 (dt, J = 7.1, 2.0 Hz, 1H), 7.45 – 7.35 (m, 2H), 4.21 (s, 2H). 13C NMR (125 MHz, DMSO-d6) δ 165.29, 138.08, 131.68, 129.51, 124.88, 121.34, 120.50, 116.90, 43.44.

***N-(2-acetylphenyl)-2-chloroacetamide* (55)**

Pale Yellow Solid (0.375g, 89.54% yield) M.P: 154-157°C, Rf=0.9 (EA/Hex,7:3,v/v). IR(ATR): 1658 (C=0 stretching), 3264(Secondary NH stretching), 2962(C-H stretching), 1222 (C-N stretching) cm^{-1}. ^{1}H NMR (500 MHz, DMSO-d6) δ 9.51 – 9.47 (NH,s, 1H), 8.41 – 8.35 (Ar-H,m, J = 8.1, 1.4 Hz, 1H), 7.82 – 7.77 (Ar-H,m, J = 8.1, 1.5 Hz, 1H), 7.56 – 7.49 (Ar-H,td, J = 7.9, 1.5 Hz, 1H), 7.24 – 7.18 (Ar-H,m, 1H), 4.23 – 4.20 (CH2,s, 2H), 2.66 – 2.63 (CH3,s, 3H). 13C NMR (125 MHz, DMSO-d6) δ 201.96, 168.03, 138.23, 133.18, 129.86, 129.71, 123.95, 122.96, 41.74, 28.28.

***N-(3-acetylphenyl)-2-chloroacetamide* (56)**

Grey Solid (0.321g, 87.33% yield) M.P: 178-181°C, Rf=0.79 (EA/Hex,7:3,v/v). IR(ATR) : 1646 (C=0 stretching), 3226(Secondary NH stretching), 2956(C-H stretching), 1182 (C-N stretching) cm^{-1}. ^{1}H NMR (500 MHz, DMSO-d6) δ 9.38 – 9.34 (NH,s, 1H), 8.00 – 7.96 (Ar-H,t, J = 2.2 Hz, 1H), 7.75 – 7.70 (Ar-H,m, J = 7.9, 2.2, 1.3 Hz, 1H), 7.67 – 7.61 (Ar-H,m, J = 8.0, 2.2, 1.3 Hz, 1H), 7.45 – 7.38 (Ar-H,d, J = 16.0 Hz, 1H), 4.23 – 4.19 (CH,s, 2H), 2.57 – 2.53 (CH3,s, 3H).. 13C NMR (125 MHz, DMSO-d6) δ 197.37, 167.69, 138.63, 138.05, 128.79, 126.64, 124.50, 121.11, 41.74, 27.79.

***N-(4-acetylphenyl)-2-chloroacetamide* (57)**

Grey Solid (0.403g, 90.87% yield) M.P: 167-172°C, Rf=0.88 (EA/Hex,7:3,v/v). IR(ATR) : 1651 (C=0 stretching), 3218(Secondary NH stretching), 2967(C-H stretching), 1188 (C-N stretching) cm^{-1}. ^{1}H NMR (500 MHz, DMSO-d6) δ 9.18 – 9.14 (NH,s, 1H), 7.89 – 7.83 (Ar-H,m, 2H), 7.54 – 7.48 (Ar-H,m, 2H), 4.23 – 4.19 (CH2,s, 2H), 2.60 – 2.56 (CH3,s, 3H). 13C NMR (125 MHz, DMSO-d6) δ 197.14, 167.69, 143.26, 131.62, 130.19, 119.59, 41.74, 27.79.

6.3.4.2 General procedure for the synthesis of *N-benzyl piperidine* analogues

Aniline intermediate (1 equivalent) was dissolved in Acetonitrile (10 ml) containing Triethylamine (2 equivalent) and 4-Amino benzyl piperidine (1 equivalent). The reaction mixture was heated up to 70℃ for 6 h, followed by a workup with water-ethylacetate system and the organic layer was evaporated under reduced pressure through a rotary evaporator. The product formed was checked through TLC using the ethylacetate and hexane (7:3) as the mobile phase. The product was purified by column chromatography using ethylacetate and hexane as a mobile phase.

***2-((1-benzylpiperidin-4-yl) amino)-N-phenylacetamide* (59)**

White solid (0.15g, 65.36% yield). M.P: 152-155°C,R_f =0.42 (EA/Hex,7:3,v/v). IR (ATR): 1649(C=0 stretching), 3271(Secondary NH stretching), 2962(C-H stretching), 1214(C-N stretching) cm^{-1}. ^{1}H NMR (500 MHz, DMSO-d6) δ 8.99 – 8.96 (CONH,s, 1H), 7.55 – 7.49 (Ar-H,m, 2H), 7.47 – 7.40 (Ar-H,m, 2H), 7.33 – 7.23 (Ar-H,m, 5H), 7.17 – 7.11 (Ar-H,m, J = 6.9, 1.1 Hz, 1H), 3.56 – 3.53 (CH2,s, 2H), 3.49 – 3.44 (CH2,d, J = 5.8 Hz, 2H), 3.40 – 3.32 (NH,m, J = 7.1, 6.0, 5.3 Hz, 1H), 3.02 – 2.94 (CH,dp, J = 7.1, 4.1 Hz, 1H), 2.80 – 2.71 (CH2,m, J = 12.6, 8.1, 5.4 Hz, 2H), 2.53 – 2.44 (CH2,m, J = 12.8, 8.2, 5.5 Hz, 2H), 1.96 – 1.86 (CH2,m, J = 12.5, 8.2, 5.5, 4.2 Hz, 2H), 1.69 – 1.59 (CH2,m, 2H). ^{13}C NMR (125 MHz, DMSO-d6) δ 168.41, 138.23, 137.76, 129.42, 128.92, 128.14,

126.55, 123.72, 121.57, 63.66, 58.62, 51.44, 50.81, 30.97. MS (EI+): m/z calculated for $C_{20}H_{25}N_3O$ 324.2031, found - 324.2028 $(M+H)^+$.

***2-((1-benzylpiperidin-4-yl)amino)-N-(2-nitrophenyl)acetamide* (60)**

Yellow Solid (0.230 g, 61.66% yield) M.P: 160-164°C, Rf=0.39 (EA/Hex,7:3,v/v). IR(ATR): 1664(C=0 stretching), 3148(Secondary NH stretching), 2921(C-H stretching), 1175(C-N stretching) cm^{-1}.^{1}H NMR (500 MHz, DMSO-d6) δ 9.75 – 9.71 (CONH,s, 1H), 8.51 – 8.46 (Ar-H,m, J = 7.7, 1.4 Hz, 1H), 8.28 – 8.22 (Ar-H,m, J = 9.0, 1.4 Hz, 1H), 7.75 – 7.68 (Ar-H,td, J = 7.6, 1.3 Hz, 1H), 7.42 – 7.35 (Ar-H,m, J = 9.2, 7.9, 1.4 Hz, 1H), 7.33 – 7.23 (Ar-H,m, 5H), 3.56 – 3.51 (CH2,m, 4H), 3.40 – 3.32 (NH,m, J = 7.3, 5.8 Hz, 1H), 3.02 – 2.94 (CH,dp, J = 7.1, 4.1 Hz, 1H), 2.80 – 2.71 (CH2,m, J = 12.6, 8.1, 5.4 Hz, 2H), 2.53 – 2.44 (CH2,m, J = 12.8, 8.2, 5.5 Hz, 2H), 1.96 – 1.86 (CH2,m, J = 12.5, 8.2, 5.5, 4.2 Hz, 2H), 1.69 – 1.59 (CH2,m, 2H). 13C NMR (125 MHz, DMSO-d6) δ 167.99, 138.23, 136.51, 135.90, 133.67, 128.81, 127.95, 127.13, 126.55, 124.07, 63.66, 58.62, 51.25, 50.81, 30.87. MS (EI+): m/z calculated for $C_{20}H_{24}N_4O_3$ 369.1882, found 369.1892 $[M+H]^+$.

***2-((1-benzylpiperidin-4-yl)amino)-N-(3-nitrophenyl)acetamide* (61)**

Pale Yellow Solid (0.262 g, 63.53% yield)M.P: 179-185°C, Rf=0.49 (EA/Hex,7:3,v/v). IR(ATR) : 1670(C=0 stretching),3247(Secondary NH stretching),2954(C-H stretching),1197(C-N stretching) cm^{-1}.^{1}H NMR (500 MHz, DMSO-d6) δ 9.94 – 9.91 (CONH,s, 1H), 8.52 – 8.48 (Ar-H,t, J = 2.2 Hz, 1H), 8.46 – 8.40 (Ar-H,m, J = 7.9, 1.9, 1.0 Hz, 1H), 7.76 – 7.70 (Ar-H,m, J = 7.9, 2.4, 0.9 Hz, 1H), 7.60 – 7.53 (Ar-H,m, 1H), 7.33 – 7.23 (Ar-H,m, 5H), 3.56 – 3.53 (CH2,s, 2H), 3.49 – 3.44 (d, J = 5.8 Hz, 2H), 3.40 – 3.32 (NH,m, J = 7.1, 6.0, 5.3 Hz, 1H), 3.02 – 2.94 (CH,dp, J = 7.1, 4.1 Hz, 1H), 2.80 – 2.71 (CH2,m, J = 12.6, 8.1, 5.4 Hz, 2H), 2.53 – 2.44 (CH2,m, J = 12.8, 8.2, 5.5 Hz, 2H), 1.96 – 1.86 (CH2,m, J = 12.5, 8.2, 5.5, 4.2 Hz, 2H), 1.69 – 1.59 (CH2,m, 2H). 13C NMR

(125 MHz, DMSO-d6) δ 168.41, 148.70, 139.64, 138.23, 129.27, 128.81, 127.95, 127.01, 126.55, 120.28, 115.89, 63.66, 58.62, 51.25, 50.81, 30.87. MS (EI+): m/z calculated for $C_{20}H_{24}N_4O_3$ 369.1882, found 369.1869 $[M+H]^+$.

***2-((1-benzylpiperidin-4-yl)amino)-N-(4-nitrophenyl)acetamide* (62)**

Yellow Solid (0.256g, 62.71% yield) M.P: 170-173°C, Rf=0.4 (EA/Hex,7:3,v/v). IR(ATR): 1644(C=0 stretching),3267(Secondary NH stretching),2924(C-H stretching),1173(C-N stretching) cm^{-1}.^{1}H NMR (500 MHz, DMSO-d6) δ 9.64 – 9.60 (CONH,s, 1H), 8.22 – 8.16 (Ar-H,m, 2H), 7.83 – 7.77 (Ar-H,m, 2H), 7.33 – 7.23 (Ar-H,m, 5H), 3.56 – 3.52 (CH2,d, J = 0.7 Hz, 2H), 3.49 – 3.44 (CH2,d, J = 5.7 Hz, 2H), 3.40 – 3.32 (NH,m, J = 7.1, 6.0, 5.3 Hz, 1H), 3.02 – 2.94 (CH,dp, J = 7.1, 4.1 Hz, 1H), 2.80 – 2.71 (CH2,m, J = 12.6, 8.1, 5.4 Hz, 2H), 2.53 – 2.44 (CH2,m, J = 12.8, 8.2, 5.5 Hz, 2H), 1.96 – 1.86 (CH2,m, J = 12.6, 8.2, 5.5, 4.2 Hz, 2H), 1.69 – 1.59 (CH2,m, 2H). 13C NMR (125 MHz, DMSO-d6) δ 168.41, 145.42, 144.14, 138.23, 128.81, 127.95, 126.55, 125.54, 120.66, 63.66, 58.62, 51.25, 50.81, 30.87. MS (EI+): m/z calculated for $C_{20}H_{24}N_4O_3$ 369.1882, found- 369.1909 $[M+H]^+$.

***2-((1-benzylpiperidin-4-yl)amino)-N-(2-bromophenyl)acetamide* (63)**

White Solid (0.173g, 68.41% yield) M.P: 150-154°C, Rf=0.4 (EA/Hex,7:3,v/v). IR(ATR) : 1642(C=0 stretching),3233(Secondary NH stretching),2954(C-H stretching),1178(C-N stretching) cm^{-1}.^{1}H NMR (500 MHz, DMSO-d6) δ 9.52 – 9.48 (CONH,s, 1H), 7.69 – 7.64 (Ar-H,m, J = 7.7, 1.4 Hz, 1H), 7.56 – 7.50 (Ar-H,m, J = 8.1, 1.4 Hz, 1H), 7.35 – 7.20 (Ar-H,m, 7H), 3.56 – 3.50 (CH2,m, 4H), 3.40 – 3.32 (NH,m, J = 7.2, 5.8 Hz, 1H), 3.02 – 2.94 (CH,dp, J = 7.1, 4.1 Hz, 1H), 2.80 – 2.71 (CH2,m, J = 12.6, 8.1, 5.4 Hz, 2H), 2.53 – 2.44 (CH2,m, J = 12.8, 8.2, 5.5 Hz, 2H), 1.96 – 1.86 (CH2,m, J = 12.5, 8.2, 5.5, 4.2 Hz, 2H), 1.69 – 1.59 (CH2,m, 2H). 13C NMR (125 MHz, DMSO-d6) δ 167.99, 138.33, 138.23, 133.51, 128.81, 128.47, 127.95, 126.55, 125.51, 123.39, 113.90, 63.66, 58.62,

51.25, 50.81, 30.87. MS (EI+): m/z calculated for $C_{20}H_{24}BrN_3O$ 402.1181, found - 402.1169 $[M+H]^+$.

2-((1-benzylpiperidin-4-yl)amino)-N-(3-bromophenyl)acetamide **(64)**

White Solid (0.166, 67.60% yield) M.P: 180-183°C, Rf=0.39 (EA/Hex,7:3,v/v). IR(ATR): 1654(C=0 stretching), 3367 (Secondary NH stretching), 2977(C-H stretching),1184 (C-N stretching) cm^{-1}. ^1H NMR (500 MHz, DMSO-d6) δ 9.52 – 9.48 (CONH,s, 1H), 7.69 – 7.64 (Ar-H,m, J = 7.7, 1.4 Hz, 1H), 7.56 – 7.50 (Ar-H,m, J = 8.1, 1.4 Hz, 1H), 7.35 – 7.20 (Ar-H,m, 7H), 3.56 – 3.50 (CH2,m, 4H), 3.40 – 3.32 (NH,m, J = 7.2, 5.8 Hz, 1H), 3.02 – 2.94 (CH,dp, J = 7.1, 4.1 Hz, 1H), 2.80 – 2.71 (CH2,m, J = 12.6, 8.1, 5.4 Hz, 2H), 2.53 – 2.44 (CH2,m, J = 12.8, 8.2, 5.5 Hz, 2H), 1.96 – 1.86 (CH2,m, J = 12.5, 8.2, 5.5, 4.2 Hz, 2H), 1.69 – 1.59 (CH2,m, 2H). 13C NMR (125 MHz, DMSO-d6) δ 168.41, 139.30, 138.23, 130.42, 128.81, 127.95, 127.62, 122.67, 121.91, 120.63, 63.66, 58.62, 51.25, 50.81, 30.87. MS (EI+): m/z calculated for $C_{20}H_{24}BrN_3O$ 402.1181, found 401.1174 $[M+H]^+$.

2-((1-benzylpiperidin-4-yl)amino)-N-(4-bromophenyl)acetamide **(65)**

White Solid (0.192, 63.72% yield) M.P:176-178°C, Rf=0.36 (EA/Hex, 7:3,v/v). IR(ATR): 1658(C=0 stretching),3255(Secondary NH stretching),2977(C-H stretching),1187(C-N stretching) cm^{-1}.^1H NMR (500 MHz, DMSO-d6) δ 9.58 – 9.54 (CONH,s, 1H), 7.53 – 7.43 (Ar-H,m, 4H), 7.33 – 7.23 (Ar-H,m, 5H), 3.56 – 3.52 (CH2,d, J = 0.7 Hz, 2H), 3.49 – 3.44 (CH2,d, J = 5.7 Hz, 2H), 3.40 – 3.32 (NH,m, J = 7.1, 6.0, 5.3 Hz, 1H), 3.02 – 2.94 (CH,dp, J = 7.1, 4.1 Hz, 1H), 2.80 – 2.71 (CH2,m, J = 12.6, 8.1, 5.4 Hz, 2H), 2.53 – 2.44 (CH2,m, J = 12.8, 8.2, 5.5 Hz, 2H), 1.96 – 1.86 (CH2,m, J = 12.6, 8.2, 5.5, 4.2 Hz, 2H), 1.69 – 1.59 (CH2,m, 2H). 13C NMR (125 MHz, DMSO-d6) δ 168.41, 138.23, 136.21, 131.79, 128.81, 127.95, 126.55, 122.19, 118.25, 63.66, 58.62,

51.25, 50.81, 30.87. MS (EI+): m/z calculated for $C_{20}H_{24}BrN_3O$ 402.1181, found – 402.1156 $[M+H]^+$.

2-((1-benzylpiperidin-4-yl)amino)-N-(2-fluorophenyl)acetamide **(66)**

White Solid (0.232g,61.70% yield)M.P: 162 – 165°C, Rf=0.38 (EA/Hex,7:3,v/v). IR(ATR) : 1647(C=0 stretching),3354(Secondary NH stretching),2978(C-H stretching),1192(C-N stretching) cm^{-1}.^{1}H NMR (500 MHz, DMSO-d6) δ 9.84 (s, 1H), 8.29 – 8.19 (m, 2H), 7.89 (dd, J = 5.2, 1.1 Hz, 1H), 7.77 (d, J = 5.5 Hz, 2H), 7.71 – 7.61 (m, 2H), 7.41 (t, J = 4.6 Hz, 1H), 7.18 (t, J = 5.1 Hz, 1H), 5.13 (s, 1H), 4.68 (s, 2H), 4.37 (s, 2H), 3.14 – 3.00 (m, 4H), 2.90 (dd, J = 6.8, 3.2 Hz, 1H), 2.46 – 2.09 (m, 4H). 13C NMR (125 MHz, DMSO-d6) δ 171.63, 163.58, 140.77, 139.13, 130.89, 129.20, 127.26, 115.34, 110.09, 106.44, 62.68, 55.00, 52.22, 50.57, 32.51. MS (EI+) m/z: calculated for $C_{20}H_{24}FN_3O$ 342.1937, found - 342.1969 $[M+H]^+$.

2-((1-benzylpiperidin-4-yl)amino)-N-(3-fluorophenyl)acetamide **(67)**

White Solid (0.212g, 66.77% yield) M.P: 110-114°C, Rf=0.43 (EA/Hex,7:3,v/v). IR(ATR) : 1652(C=0 stretching),3362(Secondary NH stretching),2978(C-H stretching),1192(C-N stretching) cm^{-1}.^{1}H NMR (500 MHz, DMSO-d6) δ 9.70 – 9.67 (CONH,s, 1H), 7.50 – 7.44 (Ar-H,m, J = 7.7, 2.2, 1.1 Hz, 1H), 7.35 – 7.23 (Ar-H,m, 7H), 6.92 – 6.84 (Ar-H,m, J = 9.9, 7.7, 2.1, 1.1 Hz, 1H), 3.56 – 3.52 (CH2,d, J = 0.7 Hz, 2H), 3.49 – 3.44 (CH2,d, J = 5.7 Hz, 2H), 3.40 – 3.32 (NH,m, J = 7.1, 6.0, 5.3 Hz, 1H), 3.02 – 2.94 (CH,dp, J = 7.1, 4.1 Hz, 1H), 2.80 – 2.71 (CH2,m, J = 12.6, 8.1, 5.4 Hz, 2H), 2.53 – 2.44 (CH2,m, J = 12.8, 8.2, 5.5 Hz, 2H), 1.96 – 1.86 (CH2,m, J = 12.6, 8.2, 5.5, 4.2 Hz, 2H), 1.69 – 1.59 (CH2,m, 2H). 13C NMR (125 MHz, DMSO-d6) δ 168.41, 163.12, 140.00, 138.23, 130.05, 128.81, 127.95, 126.55, 117.04, 112.15, 109.08, 63.66, 58.62, 51.2550.81, 30.87. MS (EI+): m/z calculated for $C_{20}H_{24}FN_3O$ 342.1937, found- 341.19 $[M+H]^+$.

***2-((1-benzylpiperidin-4-yl)amino)-N-(4-fluorophenyl)acetamide* (68)**

Brown Solid (0.248g,64.27% yield) M.P: 156-162°C, Rf=0.39 (EA/Hex,7:3,v/v). IR(ATR): 1661 (C=0 stretching), 3257 (Secondary NH stretching), 2975 (C-H stretching), 1200 (C-N stretching) cm^{-1}.^{1}H NMR (500 MHz, DMSO-d6) δ 9.62 – 9.59 (CONH,s, 1H), 7.53 – 7.47 (Ar-H,m, 2H), 7.33 – 7.23 (Ar-H,m, 5H), 7.19 – 7.11 (Ar-H,m, 2H), 3.56 – 3.53 (CH2,s, 2H), 3.49 – 3.44 (CH2,d, J = 5.8 Hz, 2H), 3.40 – 3.32 (NH,m, J = 7.1, 6.0, 5.3 Hz, 1H), 3.02 – 2.94 (CH,dp, J = 7.1, 4.1 Hz, 1H), 2.80 – 2.71 (CH2,m, J = 12.6, 8.1, 5.4 Hz, 2H), 2.53 – 2.44 (CH2,m, J = 12.8, 8.2, 5.5 Hz, 2H), 1.96 – 1.86 (CH2,m, J = 12.5, 8.2, 5.5, 4.2 Hz, 2H), 1.69 – 1.59 (CH2,m, 2H). 13C NMR (125 MHz, DMSO-d6) δ 168.41, 159.97, 138.23, 134.73, 128.81, 127.95, 126.55, 122.58, 122.58, 116.47, 63.66, 58.62, 51.25, 50.81, 30.87. MS (EI+): m/z calculated for $C_{20}H_{24}FN_3O$ 342.1937, found- 342.1948 $[M+H]^+$.

***2-((1-benzylpiperidin-4-yl)amino)-N-(o-tolyl)acetamide* (69)**

White Solid (0.15g,44.93% yield) M.P: 138-142°C, Rf=0.36 (EA/Hex,7:3,v/v). IR(ATR) : 1645(C=0 stretching),3207(Secondary NH stretching),2920(C-H stretching),1217(C-N stretching) cm^{-1}.^{1}H NMR (500 MHz, DMSO-d6) δ 8.73 – 8.70 (CONH,s, 1H), 7.51 – 7.41 (Ar-H,m, 2H), 7.33 – 7.19 (Ar-H,m, 7H), 3.56 – 3.50 (CH2,m, 4H), 3.40 – 3.32 (NH,m, J = 7.2, 5.8 Hz, 1H), 3.02 – 2.94 (CH,dp, J = 7.1, 4.1 Hz, 1H), 2.80 – 2.71 (CH2,m, J = 12.6, 8.1, 5.4 Hz, 2H), 2.53 – 2.44 (CH3,m, J = 12.8, 8.2, 5.5 Hz, 2H), 1.96 – 1.86 (CH2,m, J = 12.6, 8.2, 5.5, 4.2 Hz, 2H), 1.69 – 1.59 (CH2,m, J = 12.6, 8.2, 5.5, 4.2 Hz, 2H). 13C NMR (125 MHz, DMSO-d6) δ 167.99, 138.23, 137.43, 131.80, 130.03, 128.81, 127.95, 127.54, 126.55, 124.96, 122.76, 63.66, 58.62, 51.25, 50.81, 30.87, 17.35. MS (EI+): m/z calculated for $C_{21}H_{27}N_3O$ 338.2188, found -338.2201 $[M+H]^+$.

***2-((1-benzylpiperidin-4-yl)amino)-N-(m-tolyl)acetamide* (70)**

Brown Solid (0.175 g, 52.41% yield) M.P: 165-170°C, Rf=0.38 (EA/Hex,7:3,v/v). IR(ATR) : 1650(C=0 stretching),3269(Secondary NH stretching),2921(C-H stretching),1180(C-N stretching) cm^{-1}.^{1}H NMR (500 MHz, DMSO-d6) δ 9.31 – 9.28 (CONH,s, 1H), 7.51 – 7.43 (Ar-H,m, 2H), 7.33 – 7.23 (Ar-H,m, 5H), 7.19 – 7.12 (Ar-H,t, J = 7.6 Hz, 1H), 6.97 – 6.91 (Ar-H,m, 1H), 3.56 – 3.53 (CH2,s, 2H), 3.49 – 3.44 (CH2,d, J = 5.8 Hz, 2H), 3.40 – 3.32 (NH,m, J = 7.1, 6.0, 5.3 Hz, 1H), 3.02 – 2.94 (CH,dp, J = 7.1, 4.1 Hz, 1H), 2.80 – 2.71 (CH2,m, J = 12.6, 8.1, 5.4 Hz, 2H), 2.53 – 2.44 (CH3,m, J = 12.8, 8.2, 5.5 Hz, 2H), 1.96 – 1.86 (CH2,m, J = 12.5, 8.2, 5.5, 4.2 Hz, 2H), 1.69 – 1.59 (CH2,m, J = 12.5, 8.2, 5.5, 4.2 Hz, 2H). 13C NMR (125 MHz, DMSO-d6) δ 168.41, 139.50, 138.32, 138.23, 128.94, 128.81, 127.95, 126.55, 126.50, 120.29, 119.22, 63.66, 58.62, 51.25, 50.81, 30.87, 21.21. MS (EI+): m/z calculated for $C_{21}H_{27}N_3O$ 338.2188, found- 338.2196 $[M+H]^+$.

***2-((1-benzylpiperidin-4-yl)amino)-N-(p-tolyl)acetamide* (71)**

Brown Solid (0.160 g, 47.35% yield) M.P: 155-158°C, Rf=0.43 (EA/Hex,7:3,v/v). IR(ATR) : 1648(C=0 stretching),3284(Secondary NH stretching),2978(C-H stretching),1182(C-N stretching) cm^{-1}.^{1}H NMR (500 MHz, DMSO-d6) δ 9.56 – 9.52 (CONH,s, 1H), 7.45 – 7.39 (Ar-H,m, 2H), 7.33 – 7.23 (Ar-H,m, 5H), 7.16 – 7.10 (Ar-H,m, 2H), 3.56 – 3.53 (CH2,s, 2H), 3.49 – 3.44 (CH2,d, J = 5.8 Hz, 2H), 3.40 – 3.32 (NH,m, J = 7.1, 6.0, 5.3 Hz, 1H), 3.02 – 2.94 (CH,dp, J = 7.1, 4.1 Hz, 1H), 2.80 – 2.71 (CH2,m, J = 12.6, 8.1, 5.4 Hz, 2H), 2.53 – 2.44 (CH3,m, J = 12.8, 8.2, 5.5 Hz, 2H), 1.96 – 1.86 (CH2,m, J = 12.5, 8.2, 5.5, 4.2 Hz, 2H), 1.69 – 1.59 (CH2,m, J = 12.5, 8.2, 5.5, 4.2 Hz, 2H). 13C NMR (125 MHz, DMSO-d6) δ 168.41, 138.23, 136.58, 133.31, 129.75, 128.81, 127.95, 126.55, 119.33, 63.66, 58.62, 51.25, 50.81, 30.87, 21.13. MS (EI+): m/z calculated for $C_{21}H_{27}N_3O$ 338.2188, found- 338.2194 $[M+H]^+$.

***2-((1-benzylpiperidin-4-yl)amino)-N-(2-chlorophenyl)acetamide* (72)**

Dark Brown Solid (0.192g,71.55% yield) M.P: 167-172°C, Rf=0.47 (EA/Hex,7:3,v/v). IR(ATR) : 1651(C=0 stretching),3212(Secondary NH stretching),2921(C-H stretching),1172(C-N stretching) cm^{-1}.^{1}H NMR (500 MHz, DMSO-d6) δ 9.00 – 8.97 (CONH,s, 1H), 7.50 – 7.44 (m, J = 7.9, 1.4 Hz, 1H), 7.42 – 7.35 (m, 1H), 7.33 – 7.22 (m, 6H), 7.11 – 7.04 (m, J = 8.2, 7.1, 1.4 Hz, 1H), 3.56 – 3.50 (m, 4H), 3.40 – 3.32 (NH,m, J = 7.2, 5.8 Hz, 1H), 3.02 – 2.94 (CH,dp, J = 7.1, 4.1 Hz, 1H), 2.80 – 2.71 (m, J = 12.6, 8.1, 5.4 Hz, 2H), 2.53 – 2.44 (m, J = 12.8, 8.2, 5.5 Hz, 2H), 1.96 – 1.86 (m, J = 12.5, 8.2, 5.5, 4.2 Hz, 2H), 1.69 – 1.59 (m, 2H). 13C NMR (125 MHz, DMSO-d6) δ 167.99, 138.23, 135.66, 130.62, 128.81, 128.23, 128.05, 127.95, 126.55, 126.11, 124.73, 63.66, 58.62, 51.25, 50.81, 30.87. MS (EI+): m/z calculated for $C_{20}H_{24}ClN_3O$ 358.1686, found - 358.1671 $[M+H]^+$.

***2-((1-benzylpiperidin-4-yl)amino)-N-(3-chlorophenyl)acetamide* (73)**

Dark Brown Solid (0.24g, 72.16% yield) M.P: 168-170°C, Rf=0.35 (EA/Hex,7:3,v/v). IR(ATR) : 1646(C=0 stretching),3259(Secondary NH stretching),2975(C-H stretching),1216(C-N stretching) cm^{-1}.^{1}H NMR (500 MHz, DMSO-d6) δ 9.39 – 9.35 (CONH,s, 1H), 7.56 – 7.52 (Ar-H,t, J = 2.2 Hz, 1H), 7.47 – 7.41 (Ar-H,m, J = 8.1, 2.1, 1.2 Hz, 1H), 7.35 – 7.23 (Ar-H,m, 6H), 7.19 – 7.13 (Ar-H,m, J = 7.9, 2.2, 1.3 Hz, 1H), 3.56 – 3.53 (CH2,s, 2H), 3.49 – 3.44 (CH2,d, J = 5.8 Hz, 2H), 3.40 – 3.32 (NH,m, J = 7.1, 6.0, 5.3 Hz, 1H), 3.02 – 2.94 (CH,dp, J = 7.1, 4.1 Hz, 1H), 2.80 – 2.71 (CH2,m, J = 12.6, 8.1, 5.4 Hz, 2H), 2.53 – 2.44 (CH2,m, J = 12.8, 8.2, 5.5 Hz, 2H), 1.96 – 1.86 (CH2,m, J = 12.5, 8.2, 5.5, 4.2 Hz, 2H), 1.69 – 1.59 (CH2,m, 2H). 13C NMR (125 MHz, DMSO-d6) δ 168.41, 139.54, 138.23, 134.34, 129.90, 128.81, 127.95, 126.55, 124.84, 120.45, 120.38, 63.66, 58.62, 51.25, 50.81, 30.87. MS (EI+): m/z calculated for $C_{20}H_{24}ClN_3O$ 358.1686, found - 358.1664 $[M+H]^+$.

***2-((1-benzylpiperidin-4-yl) amino)-N-(4-chlorophenyl)acetamide* (74)**

Pale Brown Solid (0.378 g, 60.19% yield) M.P: 176-178°C, R_f=0.45 (EA/Hex,7:3,v/v). IR(ATR): 1654 (C=0stretching), 3258 (Secondary NH stretching), 2977 (C-H stretching), 1171 (C-N stretching) cm^{-1}.^{1}H NMR (500 MHz, DMSO-d6) δ 9.58 – 9.54 (CONH,s, 1H), 7.62 – 7.56 (Ar-H,m, 2H), 7.38 – 7.23 (Ar-H,m, 5H), 3.56 – 3.52 (CH2,d, J = 0.7 Hz, 2H), 3.49 – 3.44 (CH2,d, J = 5.7 Hz, 2H), 3.40 – 3.32 (NH,m, J = 7.1, 6.0, 5.3 Hz, 1H), 3.02 – 2.94 (CH,dp, J = 7.1, 4.1 Hz, 1H), 2.80 – 2.71 (CH2,m, J = 12.6, 8.1, 5.4 Hz, 2H), 2.53 – 2.44 (CH2,m, J = 12.8, 8.2, 5.5 Hz, 2H), 1.96 – 1.86 (CH2,m, J = 12.6, 8.2, 5.5, 4.2 Hz, 2H), 1.69 – 1.59 (CH2,m, 2H). ^{13}C NMR (125 MHz, DMSO-d6) δ 168.41, 138.23, 136.53, 129.24, 128.81, 128.63, 127.95, 126.55, 122.21, 63.66, 58.62, 51.25, 50.81,30.87. MS (EI+): m/z calculated for $C_{20}H_{24}ClN_3O$ 358.1686, found -358.1662 $[M+H]^+$.

***2-((1-benzylpiperidin-4-yl) amino)-N-(2-methoxyphenyl) acetamide* (75)**

Pale White Solid (0.318 g, 64.10% yield) M.P: 196-198°C, R_f=0.36 (EA/Hex,7:3,v/v). ^{1}H NMR (500 MHz, DMSO-d6) *δ* 8.75 (s, 1H), 8.32 (dd, *J = 7.9, 1.5 Hz*, 1H), 7.33 – 7.23 (m, 5H), 7.09 (td, *J = 8.0, 1.5 Hz*, 1H), 7.03 (td, *J = 8.0, 1.4 Hz*, 1H), 6.93 (dd, *J = 8.1, 1.5 Hz*, 1H), 3.93 (s, 3H), 3.54 (s, 2H), 3.52 (d, *J = 5.7 Hz*, 2H), 3.40 – 3.32 (m, 1H), 3.02 – 2.94 (m, 1H), 2.80 – 2.71 (m, 2H), 2.53 – 2.44 (m, 2H), 1.96 – 1.86 (m, 2H), 1.69 – 1.59 (m, 2H). ^{13}C NMR (125 MHz, DMSO-d6) *δ* 169.70, 150.12, 137.93, 129.34, 128.89, 128.82, 127.68, 122.28, 121.79, 120.79, 110.67, 62.76, 55.69, 54.72, 52.81, 50.59, 31.73. MS (EI+): m/z calculated for $C_{21}H_{27}N_3O_2$ 354.2137, found -354.2108 $[M+H]^+$.

***2-((1-benzylpiperidin-4-yl) amino)-N-(3-methoxyphenyl) acetamide* (76)**

Pale White Solid (0.401 g, 69.48% yield) M.P: 197-199°C, R_f=0.37 (EA/Hex,7:3,v/v) ^{1}H NMR (500 MHz, DMSO-d6) *δ* 9.48 (s, 1H), 7.31 – 7.26 (m, 7H), 7.24 (d, *J = 7.9 Hz*, 1H), 7.07 (dt, *J = 7.5, 1.8 Hz*, 1H), 3.82 (s, 3H), 3.54 (s, 2H), 3.47 (d, *J = 5.9 Hz*, 2H),

3.40 – 3.32 (m, 1H), 3.02 – 2.94 (m, 1H), 2.80 – 2.71 (m, 2H), 2.53 – 2.44 (m, 2H), 1.96 – 1.86 (m, 2H), 1.69 – 1.59 (m, 2H). ^{13}C NMR (125 MHz, DMSO-d6) δ 169.73, 160.33, 140.19, 137.93, 130.02, 128.89, 128.82, 127.68, 113.55, 111.24, 106.09, 62.76, 55.59, 54.72, 52.81, 50.71, 31.73. MS (EI+): m/z calculated for $C_{21}H_{27}N_3O_2$ 354.2137, found - 354.2109 (M+).

***2-((1-benzylpiperidin-4-yl) amino)-N-(4-methoxyphenyl) acetamide* (77)**

Pale White Solid (0.271 g, 60.50% yield) M.P: 199-202°C, R_f=0.42 (EA/Hex,7:3,v/v) ^{1}H NMR (500 MHz, DMSO-d6) δ 9.59 (s, 1H), 7.98 (d, *J = 8.6 Hz*, 2H), 7.33 – 7.23 (m, 5H), 6.97 (d, *J = 8.6 Hz*, 2H), 3.80 (s, 3H), 3.54 (s, 2H), 3.47 (d, *J = 5.9 Hz*, 2H), 3.40 – 3.32 (m, 1H), 3.02 – 2.94 (m, 1H), 2.80 – 2.71 (m, 2H), 2.53 – 2.44 (m, 2H), 1.96 – 1.86 (m, 2H), 1.69 – 1.59 (m, 2H). ^{13}C NMR (125 MHz, DMSO-d6) δ 169.79, 156.42, 137.93, 133.42, 128.89, 128.82, 127.68, 122.22, 112.26, 62.76, 55.35, 54.72, 52.81, 50.65, 31.73. MS (EI+): m/z calculated for $C_{21}H_{27}N_3O_2$ 354.2137, found 354.2168 $[M+H]^+$.

***2-((1-benzylpiperidin-4-yl)amino)-N-(2-cyanophenyl)acetamide* (78)**

White Solid (0.189 g, 58.45% yield) M.P: 177-182°C, Rf=0.37 (EA/Hex,7:3,v/v). IR(ATR) : 1653(C=0 stretching),3278(Secondary NH stretching),2964(C-H stretching),1175(C-N stretching) cm^{-1}.^{1}H NMR (500 MHz, DMSO-d6) δ 9.46 – 9.42 (CONH,s, 1H), 7.75 – 7.70 (Ar-H,m, J = 6.6, 1.3 Hz, 1H), 7.67 – 7.62 (Ar-H,m, J = 7.9, 1.4 Hz, 1H), 7.49 – 7.42 (Ar-H,m, J = 8.0, 6.9, 1.4 Hz, 1H), 7.33 – 7.20 (Ar-H,m, 6H), 3.56 – 3.50 (CH2,m, 4H), 3.40 – 3.32 (NH,m, J = 7.2, 5.8 Hz, 1H), 3.02 – 2.94 (CH,dp, J = 7.1, 4.1 Hz, 1H), 2.80 – 2.71 (CH2,m, J = 12.6, 8.1, 5.4 Hz, 2H), 2.53 – 2.44 (CH2,m, J = 12.8, 8.2, 5.5 Hz, 2H), 1.96 – 1.86 (CH2,m, J = 12.5, 8.2, 5.5, 4.2 Hz, 2H), 1.69 – 1.59 (CH2,m, 2H). 13C NMR (125 MHz, DMSO-d6) δ 167.99, 141.08, 138.23, 133.62, 132.59, 128.81, 127.95, 126.55, 122.41, 121.15, 117.68, 97.59, 63.66, 58.62, 51.25,

50.81, 30.87. MS (EI+): m/z calculated for $C_{21}H_{24}N_4O$ 349.1984, found 349.1972 $[M+H]^+$.

***2-((1-benzylpiperidin-4-yl)amino)-N-(3-cyanophenyl)acetamide* (79)**

White Solid (0.185g, 57.48 % yield) M.P: 175-182°C, Rf=0.44 (EA/Hex,7:3,v/v). IR(ATR): 1661(C=0 stretching), 3273(Secondary NH stretching), 2964(C-H stretching), 1184(C-N stretching) cm^{-1}.^{1}H NMR (500 MHz, DMSO-d6) δ 9.42 – 9.39 (CONH,s, 1H), 7.91 – 7.87 (Ar-H,m, 1H), 7.83 – 7.76 (Ar-H,m, 1H), 7.47 – 7.40 (Ar-H,m, 2H), 7.33 – 7.23 (Ar-H,m, 3H), 3.56 – 3.53 (CH2,s, 2H), 3.49 – 3.44 (CH2,d, J = 5.7 Hz, 2H), 3.40 – 3.32 (NH,m, J = 7.1, 6.0, 5.3 Hz, 1H), 3.02 – 2.94 (CH,dp, J = 7.1, 4.1 Hz, 1H), 2.80 – 2.71 (CH2,m, J = 12.6, 8.1, 5.4 Hz, 2H), 2.53 – 2.44 (CH2,m, J = 12.8, 8.2, 5.5 Hz, 2H), 1.96 – 1.86 (CH2,m, J = 12.5, 8.2, 5.5, 4.2 Hz, 2H), 1.69 – 1.59 (CH2,m, 2H). 13C NMR (125 MHz, DMSO-d6) δ 168.41, 139.27, 138.23, 130.61, 129.90, 128.81, 127.95, 127.19, 126.55, 123.07, 119.29, 111.12, 63.66, 58.62, 51.25, 50.81, 30.87. MS (EI+): m/z calculated for $C_{21}H_{24}N_4O$ 349.1984, found- 349.1977 $[M+H]^+$.

***2-((1-benzylpiperidin-4-yl)amino)-N-(4-cyanophenyl)acetamide* (80)**

White Solid (0.249g, 66.55% yield) M.P: 175-178°C, Rf=0.39 (EA/Hex,7:3,v/v). IR(ATR): 1656 (C=0 stretching),3 228 (Secondary NH stretching), 2962 (C-H stretching), 1199 (C-N stretching) cm^{-1}.^{1}H NMR (500 MHz, DMSO-d6) δ 9.61 – 9.57 (CONH,s, 1H), 7.75 – 7.69 (Ar-H,m, 2H), 7.64 – 7.58 (Ar-H,m, 2H), 7.33 – 7.23 (Ar-H,m, 5H), 3.56 – 3.52 (CH2,d, J = 0.7 Hz, 2H), 3.49 – 3.44 (CH2,d, J = 5.7 Hz, 2H), 3.40 – 3.32 (NH,m, J = 7.1, 6.0, 5.3 Hz, 1H), 3.02 – 2.94 (CH,dp, J = 7.1, 4.1 Hz, 1H), 2.80 – 2.71 (CH2,m, J = 12.6, 8.1, 5.4 Hz, 2H), 2.53 – 2.44 (CH2,m, J = 12.8, 8.2, 5.5 Hz, 2H), 1.96 – 1.86 (CH2,m, J = 12.6, 8.2, 5.5, 4.2 Hz, 2H), 1.69 – 1.59 (CH2,m, 2H). 13C NMR (125 MHz, DMSO-d6) δ 168.41, 140.74, 138.23, 131.79, 128.81, 127.95, 126.55, 121.81,

119.12, 105.57, 63.66, 58.62, 51.25, 50.81, 30.87. MS (EI+): m/z calculated for $C_{21}H_{24}N_4O$ 349.1984, found -349.1969 $[M+H]^+$.

***2-((1-benzylpiperidin-4-yl) amino)-N-(2-(trifluoromethyl) phenyl) acetamide* (81)**

White Solid (0.184g, 55.27% yield) M.P: 185-187°C, Rf=0.40 (EA/Hex,7:3,v/v).^{1}H NMR (500 MHz, DMSO-d6) δ 9.07 (s, 1H), 7.95 (dd, *J = 7.1, 1.5 Hz*, 1H), 7.71 (dt, *J = 10.6, 1.4 Hz*, 1H), 7.48 – 7.44 (m, 1H), 7.37 (td, *J = 7.2, 1.4 Hz*, 1H), 7.33 – 7.23 (m, 5H), 3.56 – 3.50 (m, 4H), 3.40 – 3.32 (m, 1H), 3.02 – 2.94 (m, 1H), 2.80 – 2.71 (m, 2H), 2.53 – 2.44 (m, 2H), 1.96 – 1.86 (m, 2H), 1.69 – 1.60 (m, 2H). ^{13}C NMR (125 MHz, DMSO-d6) δ 169.76, 137.93, 137.57, 129.31, 128.89, 128.82, 127.68, 127.50, 124.58, 122.13, 121.94, 120.79, 62.76, 54.72, 52.81, 50.60, 31.73. MS (EI+): m/z calculated for $C_{21}H_{24}F_3N_3O$, 392.1905, found- 392.1901 $[M+H]^+$.

***2-((1-benzylpiperidin-4-yl) amino)-N-(3-(trifluoromethyl) phenyl) acetamide* (82)**

White Solid (0.177g, 52.50% yield) M.P: 181-184°C, Rf=0.36 (EA/Hex,7:3,v/v).

^{1}H NMR (500 MHz, DMSO-d6) δ 9.48 (s, 1H), 8.08 (t, *J = 2.1 Hz*, 1H), 7.83 (dt, *J = 7.0, 1.9 Hz*, 1H), 7.45 – 7.35 (m, 2H), 7.33 – 7.23 (m, 5H), 3.54 (s, 2H), 3.47 (d, *J = 5.9 Hz*, 2H), 3.40 – 3.32 (m, 1H), 3.02 – 2.94 (m, 1H), 2.80 – 2.71 (m, 2H), 2.53 – 2.44 (m, 2H), 1.96 – 1.86 (m, 2H), 1.69 – 1.59 (m, 2H). ^{13}C NMR (125 MHz, DMSO-d6) δ 169.70, 138.91, 137.93, 131.69, 129.46, 128.89, 128.82, 127.68, 124.88, 121.34, 120.47, 116.91, 62.76, 54.72, 52.81, 50.65, 31.73. MS (EI+): m/z calculated for $C_{21}H_{24}F_3N_3O$, 392.1905, found- 392.1897 $[M+H]^+$.

***2-((1-benzylpiperidin-4-yl) amino)-N-(4-(trifluoromethyl) phenyl) acetamide* (83)**

White Solid (0.198g, 61.48% yield) M.P: 185-187°C, Rf=0.36 (EA/Hex,7:3,v/v).

^{1}H NMR (500 MHz, DMSO-d6) δ 9.57 (s, 1H), 7.75 (d, *J = 7.3 Hz*, 2H), 7.56 (dd, *J = 7.3, 1.5 Hz*, 2H), 7.33 – 7.23 (m, 5H), 3.54 (s, 2H), 3.47 (d, *J = 5.9 Hz*, 2H), 3.40 – 3.32 (m, 1H), 3.02 – 2.94 (m, 1H), 2.80 – 2.71 (m, 2H), 2.53 – 2.44 (m, 2H), 1.96 – 1.86 (m,

2H), 1.69 – 1.59 (m, 2H). ^{13}C NMR (125 MHz, DMSO-d6) δ 169.81, 139.06, 137.93, 128.89, 128.82, 127.68, 126.85, 126.81, 125.52, 122.64, 120.39, 120.33, 62.76, 54.72, 52.81, 50.65, 31.73. MS (EI+): m/z calculated for $C_{21}H_{24}F_3N_3O$, 392.1905, found-392.1890 $[M+H]^+$.

***N-(2-acetylphenyl)-2-((1-benzylpiperidin-4-yl)amino)acetamide* (84)**

Pale Pink (0.203g, 58.29% yield) M.P: 151-154°C, Rf=0.45 (EA/Hex,7:3,v/v).IR(ATR) : 1667(C=0 stretching),3367(Secondary NH stretching),2920(C-H stretching),1217(C-N stretching) cm^{-1}.^{1}H NMR (500 MHz, DMSO-d6) δ 8.41 – 8.35 (Ar-H,m, J = 8.0, 1.3 Hz, 1H), 7.82 – 7.77 (Ar-H,m, J = 8.1, 1.5 Hz, 1H), 7.56 – 7.49 (Ar-H,td, J = 7.9, 1.6 Hz, 1H), 7.33 – 7.24 (CONH,Ar-H,m, 3H), 7.24 – 7.18 (Ar-H,td, J = 7.9, 1.4 Hz, 1H), 3.56 – 3.50 (CH2,m, 4H), 3.40 – 3.32 (NH,m, J = 7.1, 5.8 Hz, 1H), 3.02 – 2.94 (CH,dp, J = 7.1, 4.1 Hz, 1H), 2.80 – 2.71 (CH2,m, J = 12.6, 8.1, 5.4 Hz, 2H), 2.66 – 2.63 (CH3,s, 3H), 2.53 – 2.44 (CH2,m, J = 12.8, 8.2, 5.5 Hz, 2H), 1.96 – 1.86 (CH2,m, J = 12.6, 8.2, 5.5, 4.2 Hz, 2H), 1.69 – 1.59 (CH2,m, 2H). 13C NMR (125 MHz, DMSO-d6) δ 201.96, 167.99, 138.23, 133.18, 129.86, 129.71, 128.81, 127.95, 126.55, 123.95, 122.96, 63.66, 58.62, 51.25, 50.81, 30.87, 28.28. MS (EI+): m/z calculated for $C_{22}H_{27}N_3O_2$, 366.2137, found-366.2121 $[M+H]^+$.

***N-(3-acetylphenyl)-2-((1-benzylpiperidin-4-yl)amino)acetamide* (85)**

Grey Solid (0.245g, 60.17% yield) M.P: 167-172°C, Rf=0.40 (EA/Hex,7:3,v/v). IR(ATR) : 1672(C=0 stretching),3354(Secondary NH stretching),2978(C-H stretching),1177(C-N stretching) cm^{-1}.^{1}H NMR (500 MHz, DMSO-d6) δ 9.61 – 9.57 (CONH,s, 1H), 7.97 – 7.92 (Ar-H,t, J = 2.1 Hz, 1H), 7.75 – 7.70 (Ar-H,m, J = 7.9, 2.2, 1.3 Hz, 1H), 7.67 – 7.61 (Ar-H,m, J = 8.0, 2.2, 1.3 Hz, 1H), 7.45 – 7.38 (Ar-H,t, J = 8.0 Hz, 1H), 7.33 – 7.23 (Ar-H,m, 3H), 3.56 – 3.52 (CH2,d, J = 0.8 Hz, 2H), 3.49 – 3.44 (CH2,d, J = 5.7 Hz, 2H), 3.40 – 3.32 (NH,m, J = 7.1, 6.0, 5.3 Hz, 1H), 3.02 – 2.94 (CH,dp, J = 7.1, 4.1 Hz, 1H), 2.80 –

2.71 (CH2,m, J = 12.6, 8.1, 5.4 Hz, 2H), 2.57 – 2.53 (CH3,s, 2H), 2.53 – 2.44 (CH2,m, J = 12.8, 8.2, 5.5 Hz, 2H), 1.96 – 1.86 (CH2,m, J = 12.6, 8.2, 5.5, 4.2 Hz, 2H), 1.69 – 1.59 (CH2,m, 2H). 13C NMR (125 MHz, DMSO-d6) δ 197.37, 168.41, 138.63, 138.23, 138.05, 128.81, 128.79, 127.95, 126.64, 126.55, 124.50, 121.11, 63.66, 58.62, 51.25, 50.81, 30.87, 27.79. MS (EI+): m/z calculated for $C_{22}H_{27}N_3O_2$ 366.2137, found- 366.2144 $[M+H]^+$.

***N-(4-acetylphenyl)-2-((1-benzylpiperidin-4-yl)amino)acetamide* (86)**

Grey Solid (0.164g, 54.35% yield) M.P: 169-174°C, Rf=0.44 (EA/Hex,7:3,v/v). IR(ATR) : 1650(C=0 stretching), 3285(Secondary NH stretching), 2961(C-H stretching),1197(C-N stretching) cm^{-1}.^{1}H NMR (500 MHz, DMSO-d6) δ 9.61 – 9.58 (CONH,s, 1H), 7.89 – 7.83 (Ar-H,m, 2H), 7.54 – 7.48 (Ar-H,m, 2H), 7.33 – 7.23 (Ar-H,m, 3H), 3.56 – 3.52 (CH2,d, J = 0.8 Hz, 2H), 3.49 – 3.44 (CH2,d, J = 5.7 Hz, 2H), 3.40 – 3.32 (NH,m, J = 7.1, 6.0, 5.3 Hz, 1H), 3.02 – 2.94 (CH,dp, J = 7.1, 4.1 Hz, 1H), 2.80 – 2.71 (CH2,m, J = 12.6, 8.1, 5.4 Hz, 2H), 2.60 – 2.56 (CH3,s, 2H), 2.53 – 2.44 (CH2,m, J = 12.8, 8.2, 5.5 Hz, 2H), 1.96 – 1.86 (CH2,m, J = 12.5, 8.2, 5.5, 4.2 Hz, 2H), 1.69 – 1.59 (CH2,m, 2H). 13C NMR (125 MHz, DMSO-d6) δ 197.14, 168.41, 143.26, 138.23, 131.62, 130.19, 128.81, 127.95, 126.55, 119.59, 63.66, 58.62, 51.25, 50.81, 30.87, 27.79. MS (EI+): m/z calculated for $C_{22}H_{27}N_3O_2$ 366.2137, found -366.2149 (M+).

6.3.5 *In-vitro* studies

6.3.5.1 *In-vitro* cholinesterase inhibitory activity

Ellman's technique was utilized to perform the *in-vitro* studies on BChE and AChE inhibition for synthesized compounds [80, 82, 105]. *Equine* BChE and *Electrophorus electricus* AChE (CAS No. 9000-81-5 and 9001-08-1) were obtained from Sigma Aldrich, while acetylthiocholine iodide (ATCI, CAS No. 1866-15-5), butyrylthiocholine

iodide (BTCI, CAS No. 1866-16-6), and 5,5′-dithiobis(2-nitrobenzoic acid) (DTNB, CAS No. 69-78-3) were purchased from Himedia.

The compounds were first tested for AChE and BChE inhibition at a concentration of 50 μM. Subsequently, the compounds showing promising % inhibition were further evaluated to determine their IC_{50}. Six concentrations of inhibitors (50, 500, 1000, 5000, 10000, and 50000 nM) were prepared from a stock solution of 1 mg/ml in methanol, with appropriate dilutions in the assay solution. The enzyme assays were carried out in phosphate buffer saline (PBS, pH 7.4).

In the assay, 10 μL of the working solutions of inhibitors and 100 μL of DTNB solution (0.005 M) prepared in PBS were mixed in a 96-well plate and incubated for 10 minutes. After incubation, 50 μL of AChE (0.5 U mL−1) or 50 μL of BChE (0.5 U mL−1) was added, followed by a further incubation of 15 minutes. Finally, 30 μL of the substrate, either ATCI (0.00235 M) or BTCI (0.00235 M) prepared in PBS, was added to the reaction mixture. The formation of the yellow-colored 5-thio-2-nitrobenzoate anion was measured at 1-minute intervals for 20 minutes at an absorbance of 415 nm using the Synergy HTX multimode reader (BioTek, USA). A blank containing 10 μL of methanol instead of the test compound was used for comparison, and the entire procedure was performed in triplicate. The IC_{50} values were determined using GraphPad Prism 5.

The enzyme kinetics analysis was carried out for compounds 34 and 37 to determine their inhibition mechanisms, using their respective IC_{50} values as a basis. To conduct the enzyme kinetic study, five different concentrations of each inhibitor were employed. For compound 34, the concentrations were 15, 30, 60, 120, and 240 nM, while for compound 37, the concentrations were 10.5, 21, 42, 84, and 168 nM. These concentrations were selected to cover two concentrations higher and two concentrations lower than the IC_{50} of each compound.

In the enzyme kinetic study, each inhibitor concentration was incubated with six different concentrations of ATCI (0.25, 1, 2, 3, 4, and 5 μM). The reaction mixture's absorbance was monitored for 25 minutes at 415 nm using the Synergy HTX multimode reader (BioTek, USA). A blank containing 10 μL of methanol instead of the test compound was used for comparison.

To determine the enzyme inhibition mechanism, the velocity of the enzyme reaction, obtained from the product formed, was utilized to calculate Vmax and Km using Michaelis-Menten nonlinear regression graph. Additionally, the Lineweaver-Burk reciprocal plots were employed to analyze the enzyme inhibition mechanism.

The Ki value, indicative of the inhibitor's binding affinity to the enzyme, was obtained from the Dixon plot of the slope of the double reciprocal Lineweaver-Burk plot against the concentrations of the test compounds. The entire enzyme kinetic assay was performed in triplicate to ensure accuracy and consistency of the results.

6.3.5.2 *In-vitro* BACE-1 inhibition assay

The identified hits were evaluated for their BACE-1 inhibition potential using a fluorescence resonance energy transfer (FRET) based BACE-1 fluorescence assay kit (Catalog No. CS0010, Sigma-Aldrich). The kit consists of fluorescent assay buffer, stop solution, substrate (7-Methoxycumarin-4-acetyl [Asn670, Lue671]-Amyloid βA4 Precursor Protein 770 Fragment 667-676-(2,4 dinitrophenyl) Lys-Arg-Arg amide trifluoroacetate salt) and BACE-1 enzyme. Different concentrations of test compounds were prepared. The fluorescence intensity was measured immediately after the addition of BACE-1 enzyme with the wavelength of excitation and emission was set at 320 nm and 405 nm, respectively. All the measurements were performed in triplicate. The percentage inhibition was calculated using the following formulae: $[(Io–Ii)/Io] \times 100$, where Io and Ii are the fluorescence intensities obtained in the absence and presence of

an inhibitor, respectively and the IC_{50} values were calculated using linear regression graph (GraphPad Prism 5.1, GraphPad Software Inc.) [106].

6.3.5.3 *In-vitro* blood-brain barrier permeation assay

Porcine brain lipid (PBL, CAS No. 475995-51-8) and dodecane were obtained from Avanti polar lipids, Alabaster and Avra Synthesis, Hyderabad, respectively. The donor and acceptor with PVDF membrane (pore size 0.45 mm) microplates (Cat No. MAIPNTR10 and MATRNPS50) were purchased from Merck Millipore. The BBB permeability was determined by the parallel artificial membrane permeation assay (PAMPA) of compounds **64, 70, 75, 77, 80** and **86** [107]. The acceptor plate was covered with 4 µL of PBL dissolved in dodecane at a concentration of 20 mg/ml. Then, it was hydrated with 200 µL of PBS at pH 7.4. To prepare the working solution of each compound, a 200-fold dilution of a 5 mg/mL stock solution in DMSO with PBS (pH 7.4) was made, resulting in a final concentration of 25 µg/ml for each compound. Afterward, 200 µL of the working solution was added to each well of the donor plate. The donor plate was placed over the acceptor plates, and the entire setup was incubated for 18 hours. To determine the compound's concentration in the acceptor, donor, and reference wells, UV spectroscopy (HTX multimode reader, BioTek, USA) was employed. Each sample was scanned at least five different wavelengths and in three independent runs.

In a previous study, the validity of this protocol was confirmed by testing nine commercial drugs (Verapamil, Diazepam, Progesterone, Atenolol, Dopamine, Lomefloxacin, Alprazolam, Chlorpromazine, and Oxazepam) with known blood-brain barrier (BBB) permeability [80].

Following formula was used to calculate the permeability-

$$P_e = C \times -ln\left(1 - \frac{[OD]_{acceptor}}{[OD]_{equilibrium}}\right)$$

$$C = \left(\frac{(V_D - V_A)}{(V_D + V_A)a \times t}\right)$$

Where $OD_{acceptor}$ is the absorbance of Acceptor Solution minus Blank, $OD_{equilibrium}$ is the absorbance of the Equilibrium Standard minus Blank, and, using an 18 hour incubation, $C = 7.72\times10^{-6}$ cm/s.

6.3.5.4 Propidium iodine displacement assay

The Propidium iodide displacement assay serves as a valuable technique for evaluating the binding of a compound to the peripheral site of AChE. This is achieved by competitively displacing propidium iodide. In the experiment, AChE (5U) was mixed with test compounds (final concentrations 10 µM and 50 µM, 150 µl) and incubated for 6 hours at 25 °C. Another set of AChE samples was incubated without the test compounds to serve as controls. Following the incubation period, propidium iodide (final concentration 1 µM, 50 µl) was added to reach a final assay volume of 200 µl. After a 10-minute incubation, the fluorescence intensity was measured using a fluorescence plate reader (BioTek Synergy HTX) with excitation and emission wavelengths set at λ_{ex} = 535 nm and λe_m = 595 nm, respectively.

The percentage inhibition was calculated by following expression: $100 - (IF_i/IF_0 \times 100)$, where IF_i and IF_0 are the fluorescence intensities with and without inhibitor, respectively. Each assay was performed in triplicates, as three separate experiments [108].

6.3.5.5 *In-vitro* $A\beta_{1-42}$ aggregation inhibition activity

The $A\beta_{1-42}$ peptide for assessing $A\beta_{1-42}$ aggregation inhibition activity through the thioflavin T assay was obtained from Sigma-Aldrich, USA. A stock solution of $A\beta_{1-42}$ (1 mg/mL) was prepared by dissolving 1 mg of the peptide in 80 µL of 1% NH_4OH and making up the volume to 1 mL with PBS 7.4. Working concentrations of $A\beta_{1-42}$ (10 µM) were then prepared using PBS 7.4.

For the self-induced $A\beta_{1-42}$ aggregation inhibition assay, $A\beta_{1-42}$ (10 μM: 2 μl) was incubated with or without test compounds (5 μM, 10 μM, and 20 μM: 2 μl) at 37 °C for 48 hours. After the incubation period, 178 μl of 20 μM thioflavin T (ThT) was added to the 96-well plates containing the samples. Blank readings were taken using PBS buffer 7.4 instead of inhibitors. Fluorescence intensity was measured at 450 nm (excitation) and 485 nm (emission) using a microplate reader. The resulting data were plotted as normalized fluorescence intensity (NFI) with or without test compounds at different concentrations [109-111].

6.3.6 *In-vivo* evaluation of compounds

6.3.6.1 Animals, housing, and materials

Wistar rats weighing between 200–250 g of both sexes were obtained from the Institute of Medical Sciences, Banaras Hindu University, Varanasi. The rats were housed at the Animal House, Department of Pharmaceutical Engineering and Technology, Indian Institute of Technology (BHU), Varanasi. The animals were kept under controlled environmental conditions with a temperature of 25 ± 2 °C, humidity of 65 ± 5% RH, and 12 h light/dark cycles. They were provided with unrestricted access to commercial feed and water. The research protocol for behavioral studies was approved by the institutional animal ethics committee under the reference number 'IIT (BHU)/IAEC/2022/008'.

6.3.6.2 Acute oral toxicity evaluation

To assess toxicity, the evaluation followed the OECD 423 guidelines [112]. Acute toxicity studies were conducted on female rats (n = 6) by administering the drugs orally. These rats were closely observed for up to 24 hours to detect any behavioral changes, seizures, diarrhea, or mortality. Subsequently, they were kept under normal observation for an additional 14 days [113]. After the 14-day period, the animals were humanely euthanized, and their organs (brain, liver, kidney, and heart) were isolated. Thin

transverse sections (10 μm thick) were obtained using a cryostat (SLEE MEV, Germany), mounted on glass slides, and stained with hematoxylin and eosin. The slides were then examined under a bright-field microscope (Magnus MLX plus) at 10X resolution to identify any potential damage to the organs [109].

6.3.6.3 Scopolamine-induced amnesia model for testing cognition enhancement in rats

The animals were segregated into nine groups, with six animals in each group. The following treatments were used in the study: (I) control, (II) SCO (5 mg/Kg), (III) SCO + compound 72 (5 mg/Kg), (IV) SCO + compound 72 (10 mg/Kg), (V) SCO + compound 72 (20 mg/Kg), (VI) SCO + compound 77 (5 mg/Kg), (VII) SCO + compound 77 (10 mg/Kg), (VIII) SCO + compound 77 (20 mg/Kg), and (IX) SCO + DNP (5 mg/Kg). DNP and SCO were dissolved in distilled water, while the investigational compounds were suspended in 0.5% SCMC prior to the administration. SCO was administered through intraperitoneal injection (i.p.) and other compounds were administered through the oral route (p.o.) using oral gavage. The compounds, except SCO, were administered for seven days, while SCO was administered on the seventh day to induce amnesia. The behavioural experiments were performed half-hour after the SCO administration [114, 115].

6.3.6.3.1 Y-maze test

The Y-maze is a device consisting of three identical wooden arms (A, B, and C) separated by a 120˚ angle. Its purpose is to assess intermediate working and spatial memory. On the seventh day of the treatment, the test compounds 72, 77, and DNP were evaluated. Initially, a training session was conducted with one arm closed off using a wooden partition. The animal was allowed to enter the maze with its head facing toward the centre. This training occurred after dosing and four hours before the test session, during which the animal explored the maze for 15 minutes.

The test session took place half an hour after the administration of SCO (the substance being tested). In this session, the previously closed arm was opened, and the rodent was free to move around the maze for five minutes. The researchers recorded the sequence of arm entries. Repeated entries in the same arm indicated memory impairment, whereas novel arm entries and spontaneous alterations in three-consecutive components (ABC, BCA, CAB, but not ABA) were considered indicators of memory improvement [116, 117].

After each session, the maze was cleaned with 70% ethanol to eliminate any potential olfactory clues that might influence subsequent results. The % spontaneous alteration was calculated as:

$$\%\, Spontaneous\ alteration = \frac{Number\ of\ alteration}{(total\ arm\ entries - 2)} \times 100$$

6.3.6.3.2 *Ex vivo* and biochemical analysis

After the experiments, the animals were euthanized, and their brains were removed. The neurochemical analysis was focused on the hippocampus and prefrontal cortex (PFC). Tissue homogenates were prepared by homogenizing the brain tissues in 10 mM phosphate-buffered saline (PBS) with a pH of 7.4. Subsequently, centrifugation was carried out at 15000 rpm for 15 minutes at 4°C to obtain the supernatant, which was used for further analysis.

ChE (Cholinesterase) activity was determined using the Ellman method, employing acetylthiocholine iodide (ATCI) and butyrylthicholine iodide (BTCI) as substrates. Initially, 10 µL of the supernatant was diluted with 100 µL of PBS, followed by the addition of freshly prepared substrate solutions (5 mM) and incubated for 5 minutes. Afterward, 1.5 mM of DTNB solution was added, and the absorbance was measured at 415 nm using a Synergy HTX multimode reader (BioTek, USA) against a blank.

The activity of the catalase (CAT) enzyme, responsible for converting harmful H_2O_2 into water and oxygen, was measured in tissue homogenates. This was achieved by mixing 10 µL of the supernatant with 150 µL of PBS, followed by the addition of 250 µL of H_2O_2 (160 mM) and incubating for 1 minute at 37°C. Then, 1.5 mL of a stopping solution containing dichromate/acetic acid (5% $K_2Cr_2O_7$/glacial acetic acid; 1:3 v/v) was added, and the reaction mixture was boiled for 15 minutes. The green color, a result of dichromate oxidation to chromic (III) sulfate, was compared with a control mixture lacking the enzyme. Absorbance was measured at 570 nm using the Synergy HTX multimode reader (BioTek, USA) against a blank.

Superoxide dismutase (SOD) activity was determined using Markland's method, based on the autoxidation of pyrogallol. In 10 µL of tissue homogenate, 200 µL of 0.1 M Tris-HCl with 1 mM EDTA at pH 8.2 were added, followed by the addition of 50 µL of 4.5 mM pyrogallol solution prepared in 1 µM HCl. Absorbance was measured after 1 minute at 325 nm wavelength using the Synergy HTX multimode reader (BioTek, USA) against a blank. A control sample without tissue supernatant was used to determine the enzyme activity. The experiments were performed in triplicates, and enzyme activities were normalized with respect to the control group.

6.3.6.4 Aβ-induced AD phenotypic model: Morris water maze test

To evaluate memory and learning impairment induced by $A\beta_{1-42}$, a neurotoxic model was employed using the Morris water maze test [11,39]. Rats (n=6) were randomly assigned to five groups: normal control (sham), $A\beta_{1-42}$ control (negative control), 72 (20 mg/kg p.o.), 77 (20 mg/kg p.o.), and DPZ (5 mg/kg p.o.). Anesthesia was induced using an i.p. injection of a ketamine and xylene mixture (90 and 9 mg/kg, respectively). Subsequently, rats were secured on a stereotaxic apparatus, and the head was fixed with ear bars after incising and retracting the scalp. Stereotaxic coordinates were set at bregma (-0.5 mm

anteroposterior, +1.2 mm mediolateral, -3.2 dorsoventral, and incision bar set at -3.3 mm) [11]. $A\beta_{1-42}$ sterile saline solution (4 μM, 5 μl) was then infused into all groups, except the sham group, using a Hamilton microsyringe at 2 μl/min. The syringe was left in place for an additional 5 minutes to prevent solution efflux. In the sham group, saline was infused instead of $A\beta_{1-42.}$

After seven days, treatment with the test drug VA10 and DPZ commenced, administered orally once a day for the next seven days. Memory and learning capacity were assessed through behavioral studies using a test apparatus divided into four quadrants filled with opaque water (25 ± 2 °C). The water maze, with dimensions of 62 cm height, 32 cm depth, and 121 cm diameter, was used. In training trials conducted over five days, the animals were placed in one quadrant, facing the wall, and given 120 seconds to locate the hidden platform (four trials per day with a 10-minute intra-trial interval). On the sixth day, before the probe trial, the platform was removed, and animals were allowed to swim for 120 seconds to assess spatial memory. Data from observed values (escape latency in training trials, time spent on the platform, and number of entries to the platform zone) were analyzed using GraphPad Prism 9.

6.3.6.5 Statistical analyses

All values were expressed as the mean ± standard error of the mean (SEM). One-way ANOVA followed by multiple comparison posthoc test was performed.

6.4 Results and discussion

6.4.1 Rationale of drug design & *in-silico* optimization

The aim of this research was to design and novel Multi-Target Directed Ligands (MTDLs) for AD utilizing *N-benzylpiperidine* scaffolds [118]. The active site of AChE is situated within a narrow gorge, reaching a depth of 20 Å, and is characterized by two crucial residues: Trp86 at the catalytic anionic site (CAS) and Trp286 at the Peripheral Anionic

Site (PAS) [119, 120]. Considering the distinctive architecture of the active site, our molecular design incorporates two aromatic systems linked by a piperidine and a flexible chain enhancer acetamide linker. This design facilitates π–π stacking interactions with the two vital residues of AChE, namely Trp86 and Trp286 . These interactions contribute to a snug fit of the ligand within the active site, promoting a more favorable free energy of complexation. The compounds for the study were designed by a hybrid pharmacophore approach and molecule generation technique (**Figure 6.3**).

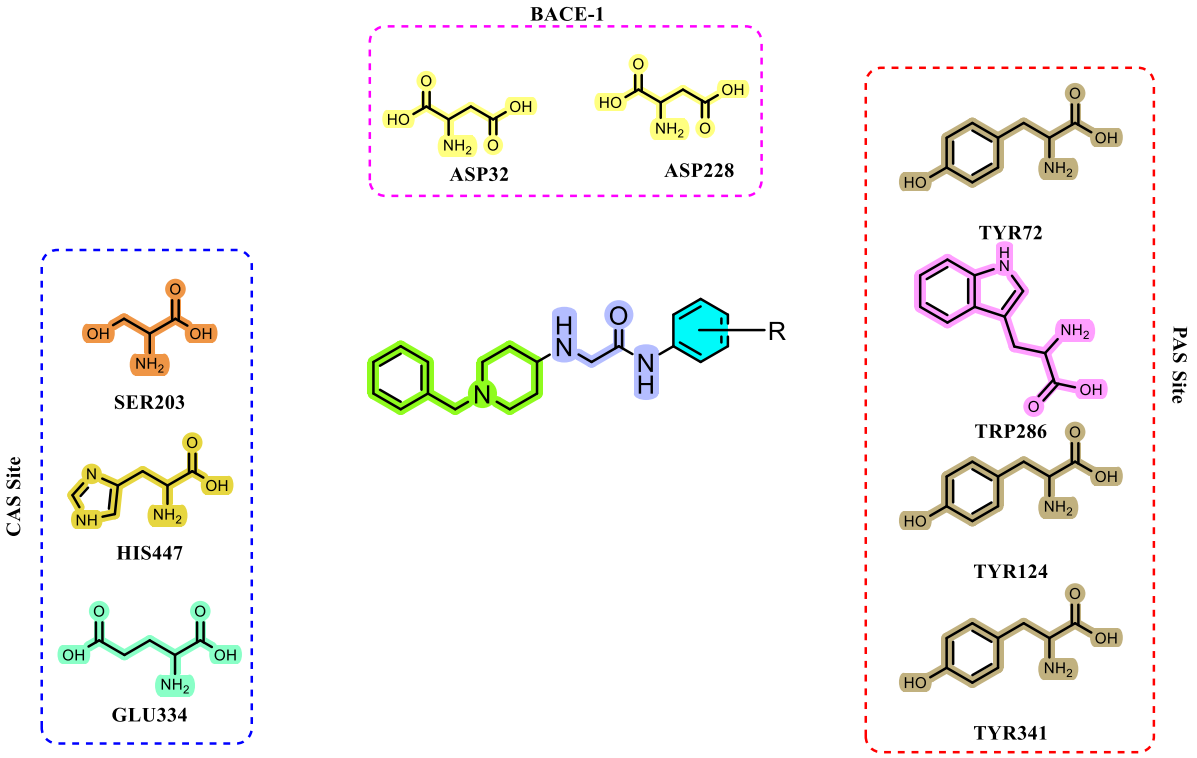

Figure 6.3 Interaction of N-benzylpiperidines with; PAS and CAS site of AChE and BACE-1.

6.4.2 Chemistry

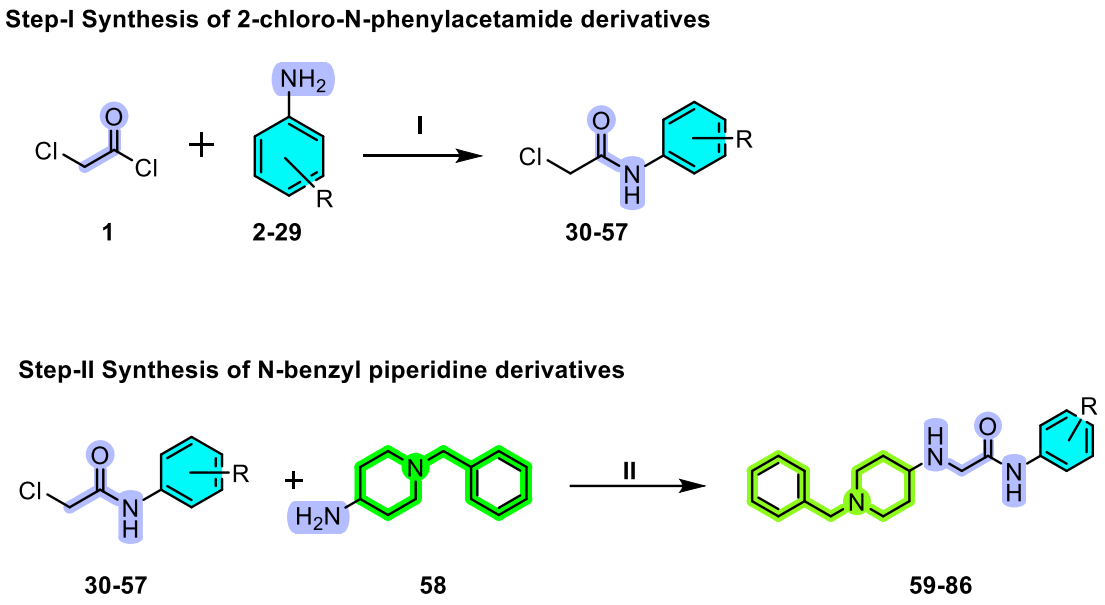

2, 30, 59 = -H
3, 31, 60 = -2NO_2
4, 32, 61 = -3NO_2
5, 33, 62 = -4NO_2
6, 34, 63 = -2Br
7, 35, 64 = -3Br
8, 36, 65 = -4Br

9, 37, 66 = -2F
10, 38, 67 = -3F
11, 39, 68 = -4F
12, 40, 69 = -2CH_3
13, 41, 70 = -3CH_3
14, 42, 71 = -4CH_3
15, 43, 72 = -2Cl

16, 44, 73 = -3Cl
17, 45, 74 = -4Cl
18, 46, 75 = -2OCH_3
19, 47, 76 = -3OCH_3
20, 48, 77 = -4OCH_3
21, 49, 78 = -2CN
22, 50, 79 = -3CN

23, 51, 80 = -4CN
24, 52, 81 = -2CF_3
25, 53, 82 = -3CF_3
26, 54, 83 = -4CF_3
27, 55, 84 = -2$COCH_3$
28, 56, 85 = -3$COCH_3$
29, 57, 86 = -4$COCH_3$

Figure 6.4 Reaction scheme (I). TEA/DCM, 1- 5 ℃, 1 hr (II). DIPEA/THF, reflux, 24hr

6.4.3 Docking studies

The docking studies with compounds 59 to 87, including DNP and CNP520, against BACE-1 (PDB ID- 6EQM) and AChE (PDB ID- 4EY7) revealed notable binding energies and ligand efficiencies. For BACE-1, the compounds exhibited binding energies ranging from -7.26 to -10.18 Kcal mol^{-1}, with corresponding ligand efficiencies between -0.29 and -0.377 Kcal mol^{-1}. Compound 72 displayed the strongest binding affinity with a remarkably low binding energy of -10.18 Kcal mol^{-1} and a ligand efficiency of -0.377 Kcal mol^{-1}. On the other hand, the interactions with AChE demonstrated binding energies from -7.27 to -9.67 Kcal mol^{-1} and ligand efficiencies between -0.269 and -0.371 Kcal mol^{-1}. Compound 77 exhibited the highest binding affinity for AChE with a binding

energy of -9.67 Kcal mol^{-1} and a ligand efficiency of -0.358 Kcal mol^{-1}. Overall, the docking results suggest that the investigated compounds have the potential to interact with both BACE-1 and AChE, indicating their possible role as dual inhibitors (**Table 6.1**).

Table 6.1 Summary of docking studies of designed compounds with AChE and BACE-1

Compound No.	**Docking result with AChE (PDB ID- 4EY7)**		**Docking result with BACE-1 (PDB ID- 6EQM)**	
	Binding energy (Kcal mol^{-1})	Ligand efficiency (Kcal mol^{-1})	Binding energy (Kcal mol^{-1})	Ligand efficiency (Kcal mol^{-1})
59	-8.38	-0.349	-7.29	-0.304
60	-8.83	-0.353	-7.86	-0.314
61	-8.73	-0.349	-7.64	-0.306
62	-8.81	-0.352	-7.55	-0.302
63	-8.65	-0.346	-8.25	-0.330
64	-9.20	-0.368	-8.08	-0.323
65	-9.04	-0.362	-7.73	-0.309
66	-8.68	-0.347	-7.40	-0.296
67	-8.27	-0.331	-7.26	-0.290
68	-8.57	-0.343	-7.21	-0.288
69	-8.95	-0.358	-7.38	-0.295
70	-9.27	-0.371	-7.51	-0.300
71	-8.84	-0.354	-8.37	-0.335
72	-7.27	-0.269	-10.18	-0.377
73	-8.02	-0.297	-8.84	-0.327
74	-8.57	-0.317	-7.83	-0.29
75	-9.16	-0.339	-8.78	-0.325
76	-8.79	-0.326	-8.65	-0.32
77	-9.67	-0.358	-8.53	-0.316
78	-9.49	-0.365	-7.44	-0.286
79	-9.29	-0.357	-8.65	-0.333
80	-9.48	-0.365	-8.28	-0.318
81	-8.06	-0.288	-7.49	-0.268
82	-8.43	-0.301	-7.35	-0.263
83	-8.43	-0.301	-7.44	-0.266
84	-9.09	-0.350	-7.28	-0.280
85	-8.29	-0.319	-7.39	-0.284
86	-8.65	-0.333	-8.15	-0.313
DNP	-8.47	-0.247	--	--
CNP520	--	--	-8.32	-0.323

6.4.4 Molecular property and toxicity prediction

The **Table 6.2** encapsulates information on diverse chemical compounds, encompassing compound ID, molecular weight, cLogP, hydrogen bond acceptors, hydrogen bond donors, and polar surface area. Noteworthy trends include a consistent count of 4 hydrogen bond acceptors and 2 hydrogen bond donors, alongside molecular weight variations. Compounds exhibit cLogP values ranging from 1.3879 to 3.1578. Notably, compounds with IDs 65 and 86 are flagged for high tumorigenicity, with compound 86 additionally marked as highly mutagenic (**Table 6.2**).

6.4.5 *In-silico* ADME prediction analysis

The **Table 6.3** provides a detailed overview of several compounds, each identified by a unique Compound ID. The compounds share commonalities in terms of their high aqueous solubility and gastrointestinal absorption, suggesting favorable characteristics for absorption in the digestive system. Moreover, all the compounds demonstrate the ability to permeate the blood-brain barrier, indicating potential central nervous system activity. In terms of enzyme inhibition, none of the compounds act as inhibitors of CYP2C9, while all of them inhibit CYP2D6 and CYP3A4. This information is crucial in understanding potential drug interactions, as these enzymes play vital roles in drug metabolism. The absence of Pan-Assay Interference Compounds (PAINS) alerts suggests that the compounds do not possess structural elements known to interfere with common screening assays, enhancing their reliability in drug development. Overall, the detailed characteristics provided in the table offer valuable insights into the pharmacological and physicochemical properties of these compounds, which can be vital for further drug development and assessment of potential therapeutic applications.

Table 6.2 Physicochemical properties and predicted toxicities of synthesized compounds

Compound ID	Mol. weight	cLogP	HA	HD	Polar Surface Area	Mutagenic	Tumorigenic
59	323.439	2.3095	4	2	44.37	None	None
60	368.436	1.3879	7	2	90.19	None	None
61	368.436	1.3879	7	2	90.19	None	None
62	368.436	1.3879	7	2	90.19	None	None
63	402.335	3.0347	4	2	44.37	None	None
64	402.335	3.0347	4	2	44.37	None	None
65	402.335	3.0347	4	2	44.37	None	High
66	341.429	2.4103	4	2	44.37	None	None
67	341.429	2.4103	4	2	44.37	None	None
68	341.429	2.4103	4	2	44.37	None	None
69	337.465	2.6534	4	2	44.37	None	None
70	337.465	2.6534	4	2	44.37	None	None
71	337.465	2.6534	4	2	44.37	None	None
72	357.884	2.9155	4	2	44.37	None	None
73	357.884	2.9155	4	2	44.37	None	None
74	357.884	2.9155	4	2	44.37	None	None
75	353.464	2.2395	5	2	53.60	None	None
76	353.464	2.2395	5	2	53.60	None	None
77	353.464	2.2395	5	2	53.60	None	None
78	348.449	2.1451	5	2	68.16	None	None
79	348.449	2.1451	5	2	68.16	None	None
80	348.449	2.1451	5	2	68.16	None	None
81	391.436	3.1578	4	2	44.37	None	None
82	391.436	3.1578	4	2	44.37	None	None
83	391.436	3.1578	4	2	44.37	None	None
84	365.475	2.1807	5	2	61.44	None	None
85	365.475	2.1807	5	2	61.44	None	None
86	365.475	2.1807	5	2	61.44	High	High

(HA- H-bond acceptor, HD- H-bond donor)

Table 6.3 *In-silico* ADME properties

Compound ID.	Aqueous solubility	GI absorption	BBB permeant	CYP2C9 inhibitor	CYP2D6 inhibitor	CYP3A4 inhibitor	PAINS alerts
59	Soluble	High	Yes	No	Yes	No	0
60	Soluble	High	No	No	Yes	Yes	0
61	Soluble	High	No	No	Yes	Yes	0
62	Soluble	High	No	No	Yes	Yes	0
63	Moderately soluble	High	Yes	No	Yes	Yes	0
64	Moderately soluble	High	Yes	No	Yes	Yes	0
65	Moderately soluble	High	Yes	No	Yes	Yes	0
66	Soluble	High	Yes	No	Yes	No	0
67	Soluble	High	Yes	No	Yes	No	0
68	Soluble	High	Yes	No	Yes	No	0
69	Soluble	High	Yes	No	Yes	No	0
70	Soluble	High	Yes	No	Yes	No	0
71	Soluble	High	Yes	No	Yes	No	0
72	Moderately soluble	High	Yes	No	Yes	Yes	0
73	Moderately soluble	High	Yes	No	Yes	Yes	0
74	Moderately soluble	High	Yes	No	Yes	Yes	0
75	Soluble	High	Yes	No	Yes	No	0
76	Soluble	High	Yes	No	Yes	Yes	0
77	Soluble	High	Yes	No	Yes	Yes	0
78	Soluble	High	Yes	No	Yes	Yes	0
79	Soluble	High	Yes	No	Yes	Yes	0
80	Soluble	High	Yes	No	Yes	Yes	0
81	Moderately soluble	High	Yes	No	Yes	Yes	0
82	Moderately soluble	High	Yes	No	Yes	Yes	0
83	Moderately soluble	High	Yes	No	Yes	Yes	0
84	Soluble	High	Yes	No	Yes	Yes	0
85	Soluble	High	Yes	No	Yes	Yes	0
86	Soluble	High	Yes	No	Yes	Yes	0

6.4.6 *In-vitro* evaluation

The summary of results against eeAChE, eqBuChe and hBACE-1 has been reported in **Table 6.4.**

Table 6.4 Inhibitory potencies of compounds against eeAChE, eqBuChE and hBCAE-1

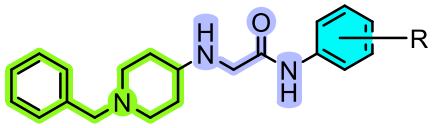

S. No	Comp.	R	eeAChE IC_{50} ± SEM (µM)	eqBuChE (% inhibition ± SEM)	hBACE-1 IC_{50} ± SEM (µM)
1	59	-H	2.144±0.083	22.46±1.079	
2	60	-2NO_2	0.165±0.04	14.63±1.053	1.384±0.064
3	61	-3NO_2	4.85±0.098	26.03±1.081	
4	62	-4NO_2	1.756±0.084	24.96±2.073	
5	63	-2Br	2.197±0.073	23.13±3.037	
6	64	-3Br	0.421±0.077	20.39±1.032	0.298±0.032
7	65	-4Br	0.804±0.075	5.620±4.074	
8	66	-2F	0.530±0.096	11.55±0.087	
9	67	-3F	4.168±0.068	17.36±2.072	
10	68	-4F	3.218±0.018	25.15±3.098	
11	69	-2CH_3	1.823±0.020	16.90±0.095	
12	70	-3CH_3	2.274±0.068	21.72±4.095	
13	71	-4CH_3	20.889±0.080	8.455±0.863	
14	72	-2Cl	0.117±0.030	19.29±3.048	0.322±0.028
15	73	-3Cl	16.206±0.075	11.90±1.025	
16	74	-4Cl	1.913±0.088	31.69±3.081	
17	75	-2OCH_3	0.413±0.010	5.325±0.560	1.936±0.144
18	76	-3OCH_3	1.168±0.079	22.98±2.054	
19	77	-4OCH_3	0.102±0.066	21.62±2.064	0.241±0.077
20	78	-2CN	0.837±0.022	12.86±1.081	
21	79	-3CN	2.819±0.084	20.70±1.065	
22	80	-4CN	0.148±0.081	27.30±0.094	0.844±0.072
23	81	-2CF_3	1.455±0.083	8.030±0.091	
24	82	-3CF_3	7.011±0.066	15.72±2.052	
25	83	-4CF_3	0.689±0.039	24.07±0.059	
26	84	-2$COCH_3$	1.609±0.079	21.42±0.062	
27	85	-3$COCH_3$	1.894±0.066	21.00±0.082	
28	86	-4$COCH_3$	0.348±0.009	7.463±4.034	2.002±0.427
29	DNP	--	0.037±0.01	26.96±2.051	

Data expressed as Mean ± SEM

6.4.6.1 Cholinesterase inhibition assay

The analysis of AChE inhibition reveals diverse trends among the tested compounds, shedding light on the structure-activity relationship (SAR). Compound 77 with a methoxy group at *para* position, stands out as a potent AChE inhibitor with a remarkably low IC_{50} of 0.102 ± 0.066 µM. Compound 60 with a nitro group at *ortho* position also showed significantly low IC_{50} of 0.165 ± 0.04 µM, suggesting that the electron-withdrawing nitro group enhances inhibitory potency. Similarly, Compound 72 containing a chloro snbstitution at *ortho* position, exhibits strong AChE inhibition with an IC_{50} of 0.117 ± 0.030 µM, emphasizing the favourable impact of certain electron-withdrawing substituents. The compounds with methyl substitution at either *ortho*, *meta*, and *para* position did not show good AChE inhibition potential as their IC_{50} values were over 1 µM.

The halogen substituents in Compounds 63, 64, 65, and 72 show diverse effects on AChE inhibition. While the Compound 63 with bromo substitution on *ortho* position and Compound 65 with bromo substitution at *para* position exhibit moderate inhibition whereas, Compound 64 having bromo substitution at *meta* position and Compound 72 with chloro substitution *ortho* position at demonstrate stronger inhibitory effects, suggesting a structural dependency on halogen substituents.

Each compound's unique structure contributes to its specific inhibitory activity against AChE, illustrating the complex interplay between R groups and inhibitory potency. These observations underscore the importance of considering both electron-withdrawing and electron-donating substituents in designing AChE inhibitors and offer valuable insights for further drug development efforts in the context of neurodegenerative disorders.

The 2D interaction diagram of Compound 60, 64, 72, 77 and 80 with crustal structure of AChE (PDB ID- 4ey7) has been shown in **Figure 6.6.** The interaction diagram shows the interaction of the selected ligands with important residues of AChE.

The enzyme kinetics study was performed to understand the type of inhibition. The enzyme kinetic study involved varying substrate concentrations (ranging from 0.25 to 5 mM) while maintaining a constant enzyme concentration to elucidate the mechanism of enzyme inhibition (**Figure 6.5**). The analysis utilized a double reciprocal Lineweaver-Burk plot, revealing that both compounds **72** and **77** exhibit a non-competitive mode of AChE inhibition. The converging lines in the third quadrant of the plot indicate that these inhibitors display a higher affinity for the enzyme-substrate complex ($\alpha < 1$) rather than the free enzyme (**Figure 6.5**).

To further quantify this interaction, Dixon plots were employed to determine the inhibition constants (Ki). The calculated inhibition constants for compounds **72** and **77** were found to be 171.99 and 203.02 nM, respectively, as illustrated in **Figure 6.5**. This data provides valuable insights into the inhibitory mechanism and potency of these compounds against AChE, emphasizing their ability to interact preferentially with the enzyme-substrate complex rather than the free enzyme during the inhibition process.

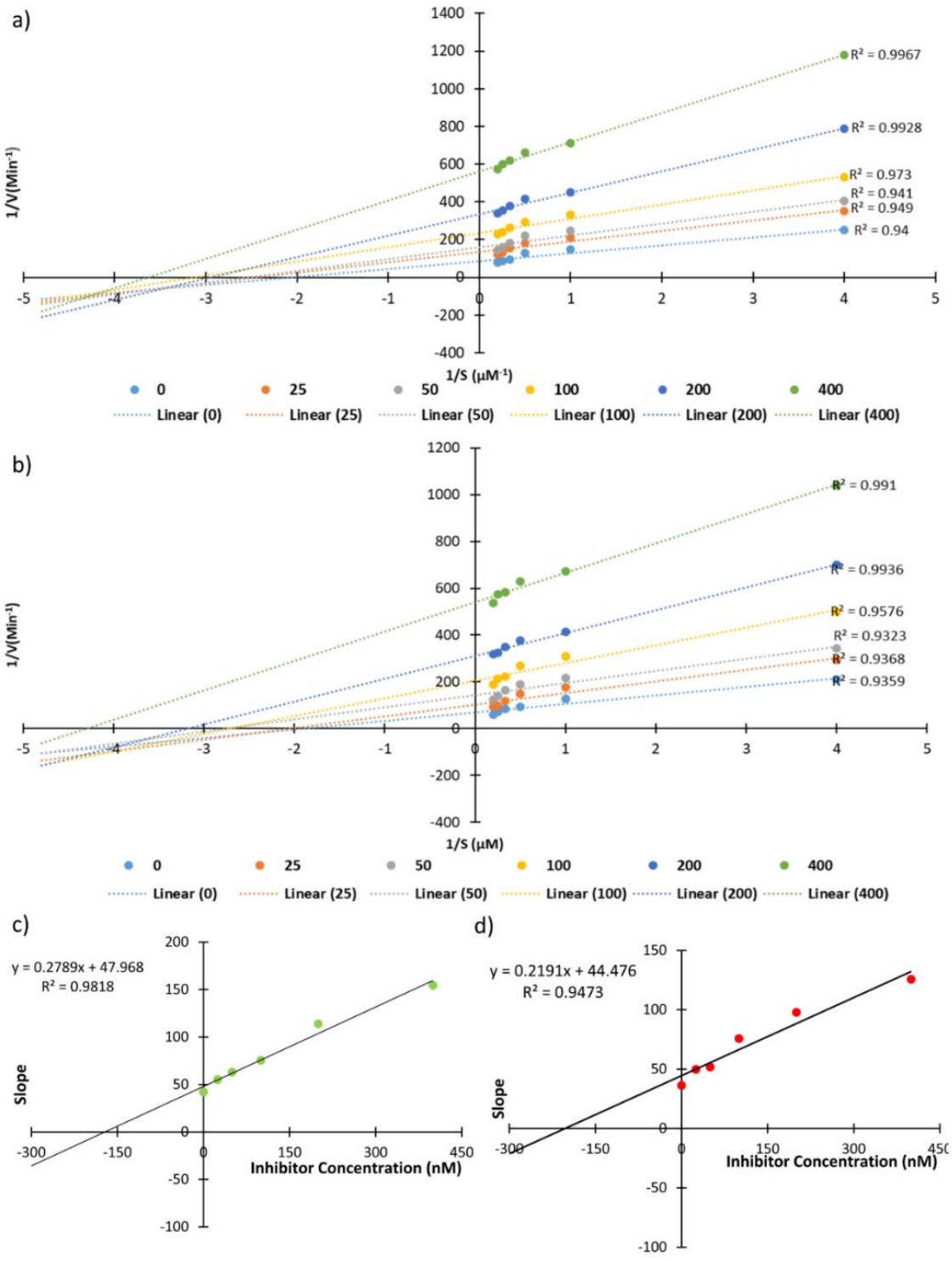

Figure 6.5 Lineweaver Burk double reciprocal plot of compounds (a) 72 and (b) 77. Dixon plot for compound (c) 72 and (d) 33 for Ki calculation

6.4.6.2 *In-vitro h*BCAE-1 inhibition assay

On the basis of AChE inhibition activity, seven compounds i.e., Compound 60, 64, 72, 75, 77, 80 and 86 were selected hBACE-1 inhibition assay. The result showed that

compound 72 and compound 77 showed good hBACE-1 inhibitory potential as compared to other five compounds (**Table 6.4**). The 2D interaction diagram of compound 72 and 77 has been shown in **Figure 6.7**. The diagrams shows interaction of ligands with important residues of BACE-1 enzyme.

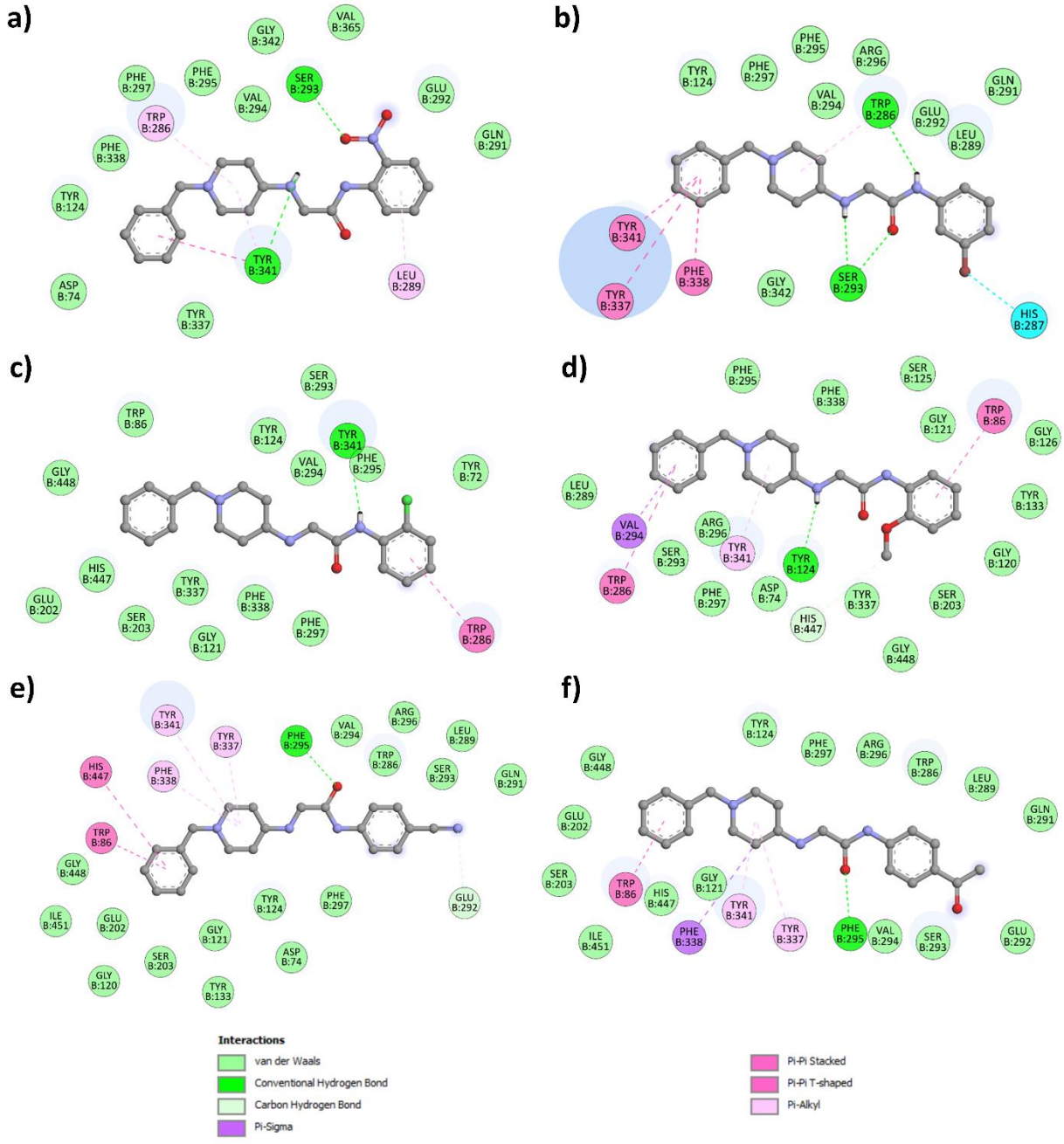

Figure 6.6 2D interaction diagram of ligands with AChE (PDB id- 4ey7). a) Compound 60, b) Compound 64, c) Compound 72, d) Compound 77, e) Compound 80 f) Compound 86

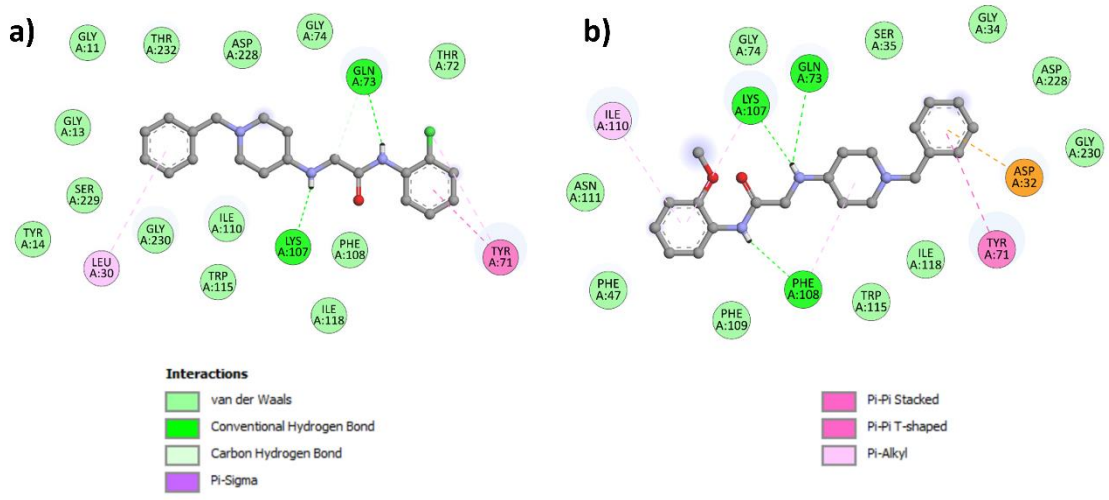

Figure 6.7 2D interaction diagram of ligands with BACE-1 (PDB id- 6eqm)

6.4.6.3 Propidium iodide (PI) displacement assay

Propidium iodide displacement assay was performed on AChE to test the ability of compounds to displace propidium with reference to the donepezil at 10 and 50 µM. Molecular docking studies revealed substantial interactions between compounds **72** and **77** and the PAS residues. Additionally, both enzyme inhibition assays and PAMPA experiments demonstrated potent inhibition of AChE and significant BBB permeation. Consequently, the binding affinity of compounds **72** and **77** to the PAS was assessed using a propidium iodide displacement assay at concentrations of 10 and 50 µM. The interaction of compounds **72** and **77** with PAS-AChE led to a reduction in fluorescence intensity. The results indicated that at 10 µM, compound **72** exhibited a 12.35% inhibition of propidium iodide displacement, while compound **77** showed a slightly higher inhibition of 15.84%. At the higher concentration of 50 µM, compound **72** demonstrated a 16.90% inhibition, and compound **77** exhibited a further increase to 21.28%. These findings suggest that both compounds exhibit a dose-dependent inhibition of propidium iodide displacement from the AChE PAS. As a reference, the standard drug donepezil

displayed a higher inhibition, with values of 19.75% at 10 µM and 32.80% at 50 µM. Overall, the results imply that compounds **72** and **77** have a notable impact on the interaction between propidium iodide and the AChE PAS, indicative of their potential as modulators of AChE function. The results obtained from the propidium iodide displacement assay align with the findings from the molecular docking studies of compounds **72** and **77 (Table 6.5)**.

Table 6.5 Propidium iodide displacement assay.

Compound	**Propidium iodide displacement from AChE PAS (% inhibition)[a]**	
	At 10 µM	At 50 µM
72	12.35 ± 1.81	16.90 ± 0.78
77	15.84 ± 2.14	21.28 ± 1.74
Donepezil	19.75 ± 2.92	32.80 ± 1.77

[a] The results are reported in Mean ± SEM (n=3)

6.4.6.4 *In-vitro* blood-brain barrier permeation assay

The PAMPA assay results provide insights into the blood-brain barrier (BBB) permeation potential of various compounds. Compound 60 exhibited a permeability value of 2.907 x 10^{-6} cm/s, suggesting a moderate likelihood of crossing the BBB (CNS±). In contrast, compounds **64, 72,** and **77** demonstrated higher permeability values of 7.435 x 10^{-6}cm/s, 5.713 x 10^{-6} cm/s, and 4.453 x 10^{-6} cm/s, respectively, indicating a positive prediction for BBB permeation (CNS+). Compound 80, with a permeability value of 1.989 x 10^{-6} cm/s, falls within the moderate range (CNS±). These findings imply that compounds 64, 72, and 77 exhibit enhanced BBB permeation potential, making them promising candidates for further investigation in the context of central nervous system drug development (**Table 6.6**).

Table 6.6 Permeability Pe (10^{-6} cm s^{-1}) data for selected potent compounds from the PAMPA-BBB assay along with their BBB Penetration prediction.

Compound code	Pe (10^{-6} cm s^{-1})	Prediction
60	2.907±0.741	CNS±
64	7.435±0.966	CNS+
72	5.713±0.620	CNS+
77	4.453±0.806	CNS+
80	1.989±0.730	CNS±

All data were expressed as Mean ± SD for experiment performed in triplicates.
Compounds with Pe > 4.324×10^{-6} cm s^{-1} could cross the BBB (CNS+), Pe < 1.846×10^{-6} cm s^{-1} could not cross the BBB (CNS−) and 1.846×10^{-6} cm s^{-1} < Pe < 4.324×10^{-6} cm s^{-1} showed uncertain BBB permeation (CNS ±).

6.4.6.5 *In-vitro* AChE induced $A\beta_{1-42}$ aggregation inhibition assay

The accumulation and aggregation of $A\beta_{1-42}$ are recognized as significant detrimental factors in AD. Findings from the PI displacement assay underscore the notable binding affinity of compounds **72** and **77** with PAS-AChE. Importantly, it is well-established that the PAS binding of the inhibitor not only leads to AChE inhibition but also plays a crucial role in preventing the aggregation of $A\beta_{1-42}$ [50]. The thioflavin T assay was employed to assess the anti-$A\beta_{1-42}$ aggregation activity of the compounds in self-induced experiments. Tests were conducted at three distinct concentration ratios of $A\beta_{1-42}$ and the inhibitor (10:5 μM, 10:10 μM, and 10:20 μM, respectively), and the results were quantified as normalized fluorescence intensity (NFI). The outcomes revealed a concentration-dependent inhibition of $A\beta_{1-42}$ aggregation, with maximum effectiveness observed at a 20 μM inhibitor concentration (**Figure 6.8**). Overall, the graph indicates that Compounds 72 and 77 exhibited concentration-dependent inhibition of Amyloid beta aggregation, with maximum inhibition at 20 μM concentration, comparable to the standard drug Donepezil. This suggests the potential of these compounds in mitigating $A\beta_{1-42}$ aggregation, a key pathological hallmark of AD.

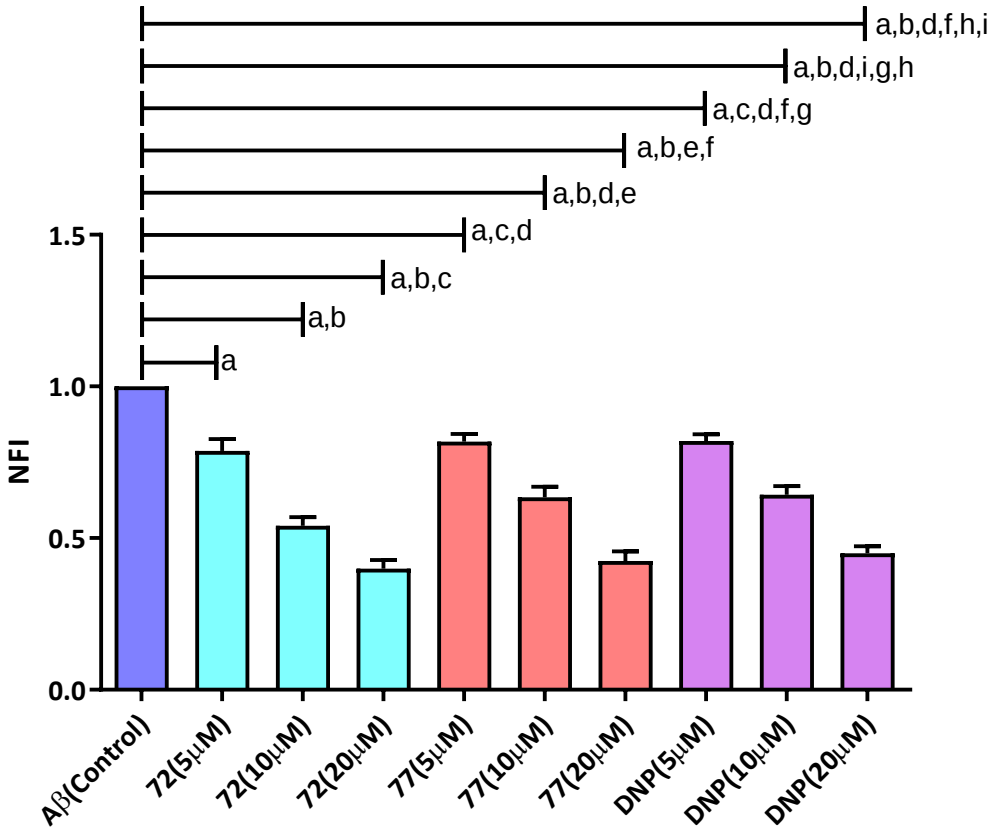

Figure 6.8 Effect of compounds 72 and 77 on $A\beta_{1-42}$ aggregation. [a] $p<0.05$ vs. Control, [b]$p<0.05$ vs. 72(5μM), [c]$p<0.05$ vs. 72(10μM), [d]$p<0.05$ vs. 72(20μM), [e]$p<0.05$ vs. 77(5μM), [f]$p<0.05$ vs. 77 (10μM), [g]$p<0.05$ vs. 77(20μM), [h]$p<0.05$ vs. DNP(5μM), [i]$p<0.05$ vs. DNP(10μM).

6.4.7 *In-Vivo* evaluation

6.4.7.1 Acute Oral Toxicity Study

Healthy female Wistar rats were used in acute oral toxicity studies to evaluate the safety of compounds **72** and **77**. The rats treated with compounds **72** and **77** did not display any signs of toxicity, such as mortality, changes in body color, weight loss, or abnormal behavior (**Table 6.7**). No significant differences were observed in biochemical parameters between the normal control group and the drug-treated rats, including creatinine, creatine kinase myocardial band (Ck-MD), alkaline phosphatase (ALP), aspartate transaminase (AST), and alanine transaminase (ALP) (**Table 6.8**). Additionally,

microscopic examination of major organs such as the brain, liver, kidney, and heart tissues revealed no adverse reactions in response to the drug therapy at doses up to 300 mg/kg when observed at 10X magnification (**Figure 6.9**).

Table 6.7 Effect of Single-Dose Oral Administration of Compound 72 and Compound 77

No. of days	Normal control (Weight in grams	Compound 72 administered rats (weight in grams)	Compound 77 administered rats (weight in grams)
0th day	214.18 ± 17.27	211.09 ± 14.25	216.49± 11.74
7th day	220.42 ± 16.36	216.38 ± 15.34	218.62± 09.16
14th day	224.76 ± 14.82	219.41 ± 14.72	222.71± 10.61

All values are expressed in Mean ± SD (n=6)

Table 6.8 Effect of Oral Administration of Compound 72 and 77

Biochemical Parameters	Normal Control	Compound 72 (300 mg/kg, po)	Compound 77 (300 mg/kg, po)
ALP (U/L)	63.64 ± 4.67	62.42 ± 2.90	64.96 ± 3.53
AST (U/L)	128.52 ± 5.31	125.25± 8.71	130.69± 4.48
ALT (U/L)	45.62 ± 3.73	47.52± 3.32	51.97 ± 4.09
Creatinine (mg/dl)	0.64 ± 0.07	0.66 ± 0.03	0.67 ± 0.14
Ck-MD (U/L)	664.47 ± 21.25	668.12 ± 19.47	661.91 ± 18.44

All values are expressed in Mean ± SD (n=6)

6.4.7.2 Scopolamine-induced amnesia model for testing cognition enhancement in rats

6.4.7.2.1 Y-maze test

The study aimed to assess the cognitive-enhancing effects of compounds **72** and **77** in comparison to the established cognitive enhancer, donepezil, using a scopolamine-induced Y-maze test in healthy male Wistar rats. Scopolamine is commonly used to induce cognitive impairment by affecting cholinergic function. The standard dose of donepezil (5 mg/kg, p.o.) and varying doses (5, 10, and 20 mg/kg, p.o.) of compounds **72** and **77** were administered to separate groups of rats for seven consecutive days. On the seventh day, scopolamine hydrobromide (0.5 mg/kg, i.p.) was administered to induce

cognitive impairment, and the Y-maze test was conducted to assess spontaneous alternations. Improved cognitive function was indicated by an increased percentage of spontaneous alternation.

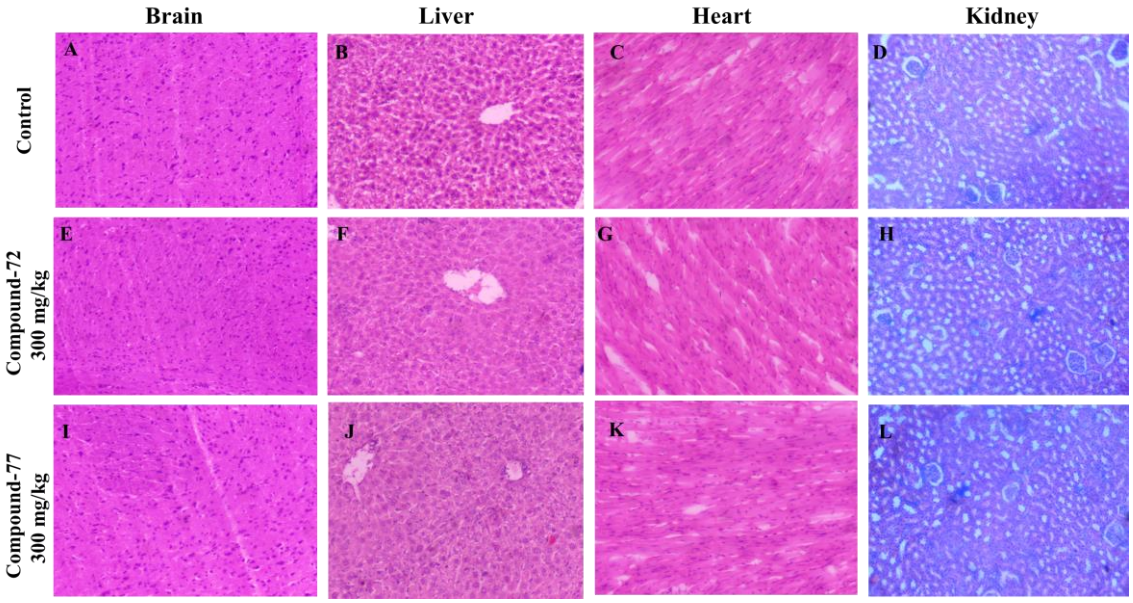

Figure 6.9 Acute oral toxicity study. Effects of the normal control group (A-D), Compound-72 (E-H) and Compound-77 (I-L) treatment on the Brain, Liver, Heart, and Kidney, respectively

Scopolamine administration led to a significant reduction in % spontaneous alternation compared to the control group, confirming the induction of cognitive deficit (Figure 5A, $p < 0.05$). Donepezil treatment exhibited significantly higher % spontaneous alternations compared to scopolamine (**Figure 6.10 (a)**, $p < 0.05$). Moreover, compounds **72** and **77** demonstrated a dose-dependent improvement in scopolamine-induced cognitive deficit, reaching maximum efficacy at 20 mg/kg. Treatment with both compounds resulted in significantly higher % spontaneous alternations compared to scopolamine, except for compound **77** at the 5 mg/kg dose (**Figure 6.10 (a)**, $p < 0.05$). Notably, at the highest dose (20 mg/kg), compounds **72** and **77** showed no statistically significant difference in % spontaneous alternation compared to donepezil (**Figure 6.10 (a),** ns).

6.4.7.2.2 *Ex-vivo* and biochemical analysis

The *ex-vivo* investigation of AChE activity was conducted using the Ellman assay, and the findings indicated a significant increase in AChE activity induced by scopolamine (**Figure 6.10 (a)**, $p < 0.05$). This elevation was attributed to extensive substrate hydrolysis compared to the control group. However, treatment with compounds **72, 77,** and donepezil exhibited notable reductions in AChE activity (**Figure 6.10 (b)**, $p < 0.05$) compared to the scopolamine-induced condition.

Furthermore, a dose-dependent elevation in acetylcholine (ACh) levels was noted in the groups treated with the drug (**Figure 6.10 (c)).** Notably, at a dose of 20 mg/kg, compound **72**, compound **77**, and donepezil exhibited no statistically significant difference in ACh levels (**Figure 6.10 (c),** ns). The behavioral and neurochemical assessment data implied that compounds **72** and **77** effectively inhibited AChE activity, leading to an increased availability of ACh in the brain.

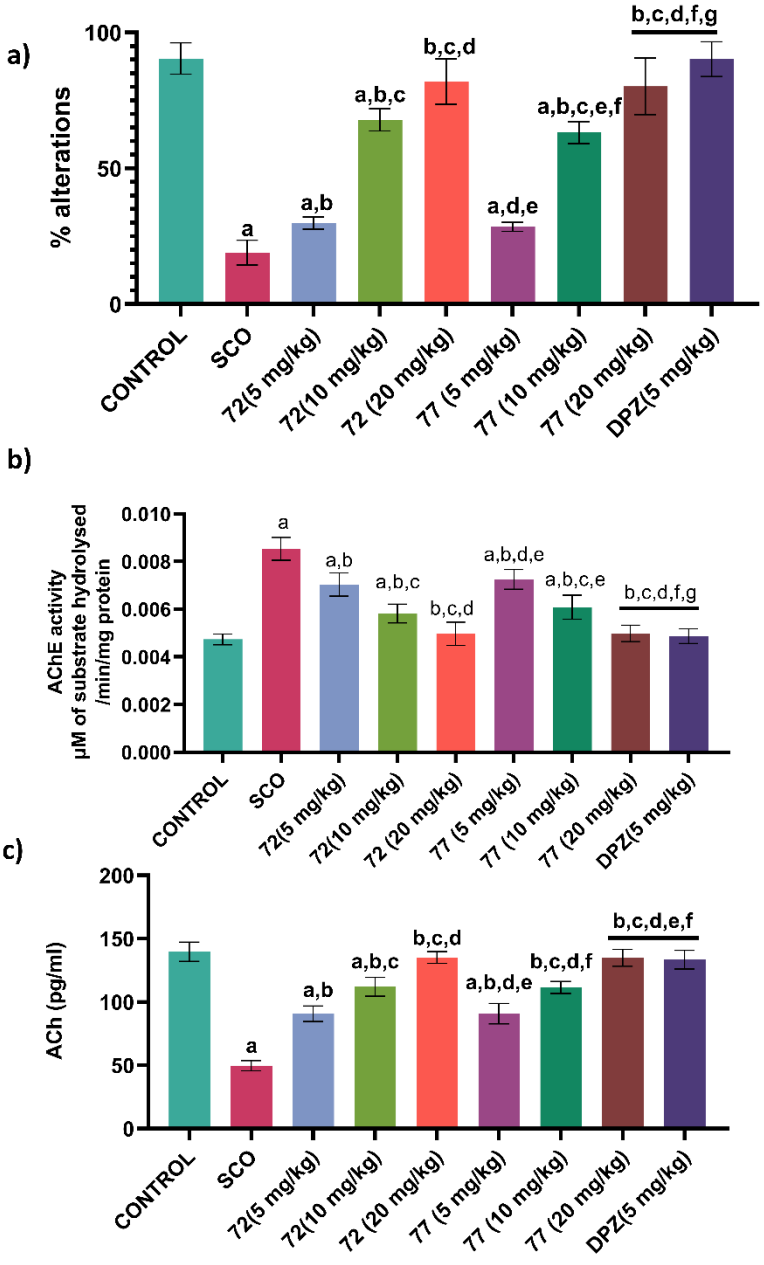

Figure 6.10 Effect of compounds 72 and 77 on scopolamine-induced cognition and memory impairment. (a) Effect of compounds 72 and 77 on % spontaneous alterations. (b) Effect of compounds 72 and 77 on AChE activity (c) Effect of compounds 72 and 77 on ACh levels. [a]p<0.05 vs. control; [b]p<0.05 vs. SCO; [c]p<0.05 vs. Compound 72 (5 mg/kg); [d]p<0.05 vs. Compound 72 (10 mg/kg); [e]p<0.05 vs. compound 72 (20 mg/kg); [f]p<0.05 vs. Compound 77 (5 mg/kg); [g]p<0.05 vs. Compound 77 (10 mg/kg) One way ANOVA followed by Newman - Keuls posthoc test. [SCO-Scopolamine]

6.4.7.3 Aβ-induced AD phenotypic model: Morris water maze test

The primary pathological condition in AD is the cerebral aggregation of $A\beta_{1-42}$. $A\beta_{1-42}$ plaques initiate toxicity and neurodegeneration by activating various biochemical cascades, such as inflammation, oxidative stress, and apoptosis, leading to the deterioration of cognitive and memory functions [121]. Cholinergic activity may decrease due to increased AChE activity around amyloid plaques. Previous studies have indicated that the accumulation of Aβ reduces ACh levels in the AD brain by upregulating the expression of AChE [122]. The intracerebroventricular injection (ICV) of $A\beta_{1-42}$ into the rat brain mimics AD-like behavior, resembling human AD [123]. $A\beta_{1-42}$ deposits cause neuronal inflammation and microglial activation, potentially resulting in learning and memory deficits in rats [124].

To assess learning and memory, behavioral studies were conducted using the Morris water maze test, i.e., escape latency time (ELT) and the time spent in the platform zone. During training trials, the escape latency time for rats decreased gradually, and the $A\beta_{1-42}$ group (negative control) took more time to find the platform (**Figure 6.11 (a)**). After completion of last training trial, memory retention was predicted by a special probe trial test, with the removal of the platform. The cognitive impairment induced by Aβ administration affirmed a significant extension of ELT (**Figure 6.11 (a**)) in the model group of animals compared to the control over 5 days. The treatment with compound **72** and **77** drastically reduced ELT compared to the model group of animals. The time spent in the platform zone was greater in the drug treated group than the $A\beta_{1-42}$ group (**Figure 6.11(b)** $P<0.05$). The compound **72** (20 mg/kg) and **77** (20 mg/kg) showed a non-significant difference (**Figure 6.11 (b),** ns) with Donepezil treated group in time spent in the platform quadrant in the probe trial.

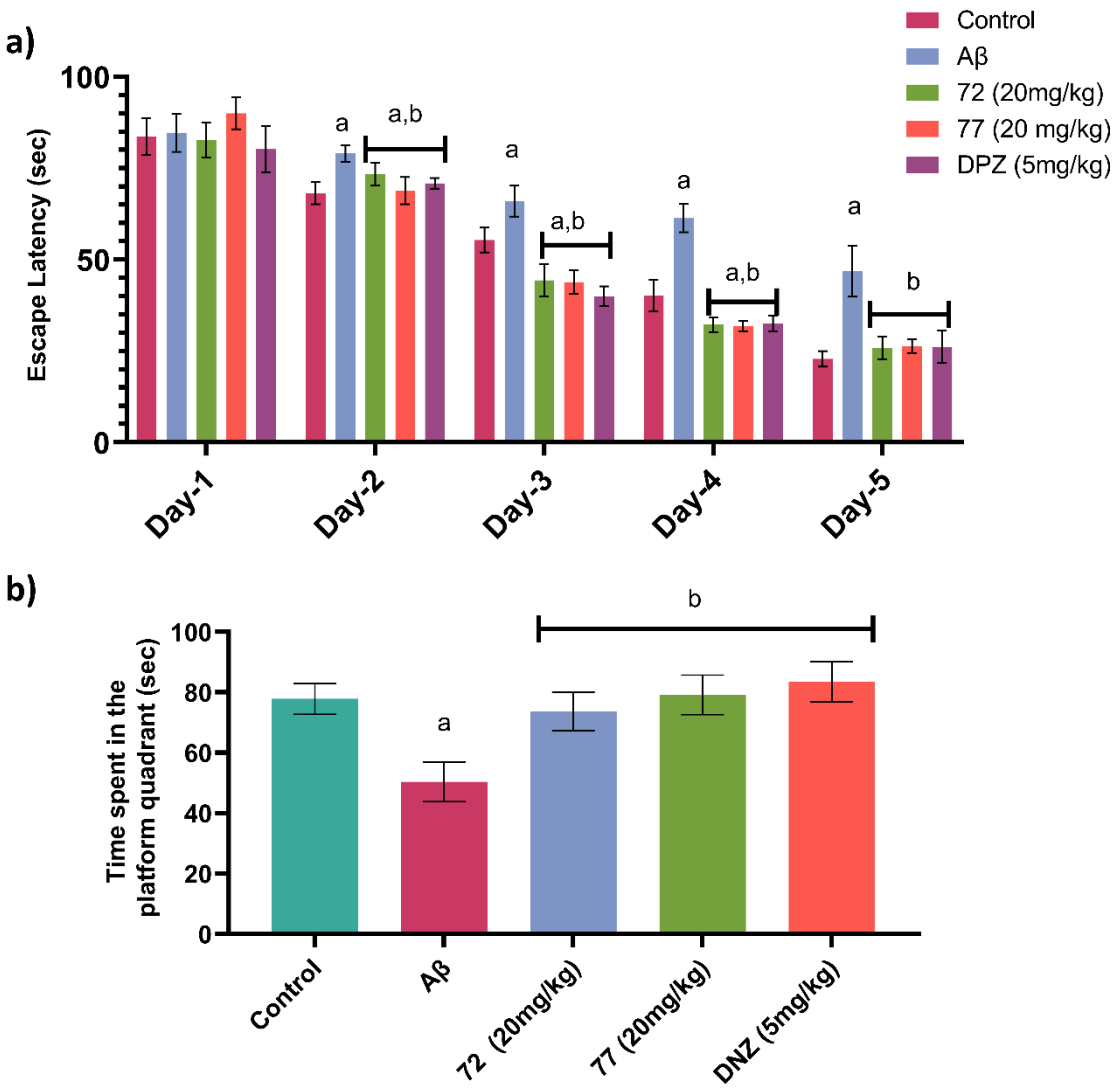

Figure 6.11 Protective effect of compounds 72, 77, and donepezil on $A\beta_{1-42}$-induced memory deficits analyzed by the Morris water maze test. (a) Escape latency during the training trials in the MWM tests; (b) time spent in the platform quadrant in the probe trial $^{a}p< 0.05$ vs. control and $^{b}p < 0.05$ vs. $A\beta_{1-42}$. One-way ANOVA followed by Newman - Keuls posthoc test.

6.5 Conclusions

This study employed a hybrid pharmacophore-based drug design approach to develop novel MTDLs targeting both AChE and BACE-1 for the treatment of AD. The design strategy focused on utilizing *N-benzylpiperidine* scaffolds to facilitate interactions with key residues in the active sites of the target enzymes. Through a combination of molecular modeling, docking studies, molecular property predictions, and *in-vitro* assays, the potential of synthesized compounds to serve as dual inhibitors of AChE and BACE-1 was evaluated.

The docking studies revealed promising binding affinities and ligand efficiencies for the designed compounds against AChE and BACE-1. Additionally, molecular property predictions indicated favorable physicochemical properties and predicted toxicities for most compounds, with certain exceptions flagged for tumorigenic and mutagenic traits. *In- silico* ADME analysis suggested good aqueous solubility, gastrointestinal absorption, and BBB permeation for most compounds, along with minimal potential for drug interactions.

In-vitro evaluation demonstrated significant inhibitory activity of the synthesized compounds against AChE, and hBACE-1, with notable structure-activity relationships observed. Compounds featuring electron-withdrawing groups exhibited enhanced inhibitory potency, while compounds with electron-donating groups showed varied inhibitory activities. Further investigation revealed mixed inhibition mechanisms for selected compounds against AChE and dose-dependent inhibition of propidium iodide displacement from the AChE PAS. Moreover, the PAMPA assay indicated several compounds' promising blood-brain barrier permeation potential.

Finally, *in-vitro* assays assessing $A\beta_{1-42}$ aggregation inhibition highlighted the potential of compounds **72** and **77** to prevent AChE-induced aggregation, suggesting their therapeutic relevance in combating AD pathology.

Overall, the findings from this study support the potential of the synthesized MTDLs as promising candidates for further development for the treatment of AD. Further preclinical and clinical studies are warranted to validate these compounds' efficacy, safety, and therapeutic potential *in-vivo*.